Comprehensive Summaries of Uppsala Dissertations
from the Faculty of Science and Technology 616

Search for Charged Higgs Bosons in e^+e^- Collisions

BY

MATTIAS ELLERT

ACTA UNIVERSITATIS UPSALIENSIS
UPPSALA 2001

Dissertation for the Degree of Doctor of Philosophy in High Energy Physics presented at Uppsala University in 2001

ABSTRACT

Ellert, M. 2001. Search for Charged Higgs Bosons in e^+e^- Collisions. Acta Universitatis Upsaliensis. *Comprehensive Summaries of Uppsala Dissertations from the Faculty of Science and Technology* 616. 68 pp. Uppsala. ISBN 91-554-4981-6.

Several extensions to the Standard Model predict the existence of charged Higgs bosons. This thesis describes the search for such a particle using the data collected by the DELPHI detector at the Large Electron Positron (LEP) collider at the European laboratory for particle physics (CERN) in Geneva, Switzerland.

In e^+e^- collisions charged Higgs bosons are predicted to be produced in pairs via an intermediate photon or Z^0 boson. In the two Higgs doublet model (2HDM) the production cross section for a pair of charged Higgs bosons depends only on the centre of mass energy of the collision and the mass of the charged Higgs boson.

Higgs bosons decay to the heaviest particles kinematically allowed. For a charged Higgs boson with a mass that can be produced at the LEP collider this means either a cs quark pair or a $\tau\nu_\tau$ lepton pair. The branching ratio between these decay channels depends on the parameters of the model.

No statistically significant signal compatible with a charged Higgs boson was found. Using the predicted production cross sections from the 2HDM the existence of a charged Higgs boson with a mass lower than 73.8 GeV/c^2 has been excluded at 95% confidence level independently of the decay branching ratios of the charged Higgs boson.

Mattias Ellert, Department of Radiation Sciences, Uppsala University, Box 535, SE-751 21 Uppsala, Sweden

ISSN 1104-232X
ISBN 91-554-4981-6

Printed in Sweden by Fyris-Tryck AB, Uppsala 2001

This thesis is based on the following papers, which will be referred to in the text by their Roman numerals:

I DELPHI Collaboration, P. Abreu *et al.*, Search for charged Higgs bosons in e^+e^- collisions at $\sqrt{s} = 172$ GeV, Phys. Lett. **B420** (1998) 140–156.

II DELPHI Collaboration, P. Abreu *et al.*, Search for Charged Higgs Bosons at LEP 2, Phys. Lett. **B460** (1999) 484–497.

III DELPHI Collaboration, P. Abreu *et al.*, Search for Charged Higgs Bosons in e^+e^- Collisions at $\sqrt{s} = 189$–202 GeV, to be submitted to Phys. Lett. **B**.

IV Mattias Ellert *et al.*, Search for Charged Higgs Bosons in e^+e^- Collisions at DELPHI, in *TAU 2000*, proceedings of the Sixth International Workshop on Tau Lepton Physics, Victoria, B.C., Canada, 18–21 September 2000, to appear in Nucl. Phys. **B**, Proc. Suppl.

V M. Battaglia *et al.*, Search for Charged Higgs Bosons in e^+e^- Collisions at $\sqrt{s} = 189$–208 GeV, contributed paper to the XXXVI$^{\mathrm{th}}$ Rencontres de Moriond, Les Arcs, France, 10–17 March 2001.

Contents

CHAPTER 1

Introduction

During the 20th century the knowledge about the laws of physics that describe the elementary particles and their interactions has increased tremendously. Today, this knowledge is summarised in the so called Standard Model that describes the electromagnetic, weak and strong interactions. The fourth fundamental interaction — gravity — is however not included in the model. Several attempts to extend the Standard Model to include gravity have been made. Some of these extensions, especially those based on supersymmetry, predict the existence of charged Higgs bosons. If a charged Higgs boson was found it would indicate the existence of new physical phenomena that are not described by the Standard Model.

When I started my Ph.D. studies in the Summer of 1996, I joined the DELPHI collaboration. This collaboration, consisting of more than 500 physicists from more than 20 countries, was responsible for the running of the DELPHI detector at the Large Electron Positron (LEP) collider at the European laboratory for particle physics (CERN) in Geneva, Switzerland. Within the collaboration, I have used the data collected by the detector to search for charged Higgs bosons. This thesis is based on this search.

The outline of the thesis is as follows:

- Chapter 2 gives the theoretical motivation for the search and introduces the two Higgs doublet model.
- Chapter 3 describes the Large Electron Positron collider and the DELPHI detector.

- Chapter 4 talks about some of the analysis methods used in the search.
- Chapter 5 gives a summary of the papers on which this thesis is based.
- Chapter 6 looks beyond the DELPHI detector and talks briefly about searches for charged Higgs bosons performed at other detectors and at other colliders.
- Appendix A gives a short summary of the Standard Model. The notation introduced in this appendix is used in other parts of the thesis as well.

Mattias Ellert
Uppsala, April 2001

CHAPTER 2

Theory

Many predictions of the Standard Model have been verified by various experiments to a remarkable precision. However, the part of the theory known as the Higgs sector, i.e. the Higgs fields and their couplings, has not been tested. In particular, the existence of the neutral Higgs boson predicted by the model has not been experimentally confirmed.

In the Standard Model the Higgs sector consists of one complex Higgs doublet field. This is the simplest choice that allows the Higgs mechanism to generate the masses of the gauge bosons of the weak interaction ($\mathrm{W}^{\pm}$ and Z^0). It is however not the only choice — the Higgs mechanism can generate masses also from other kinds of Higgs multiplet fields (e.g. triplets or quadruplets) or can use more than one Higgs multiplet field.

A model with a different or extended Higgs sector can not be considered to be an alternative to the Standard Model if its predictions are contradicted by experimental results. The two most important experimental results that impose constraints on the structure of the Higgs sector are that the ρ parameter, defined as

$$\rho \equiv \frac{m^2_{\mathrm{W}^{\pm}}}{m^2_{\mathrm{Z}^0} \cos^2\theta_{\mathrm{w}}} \ , \tag{2.1}$$

is very close to 1, and that the limits on the existence of flavour changing neutral currents, i.e. couplings between a neutral boson field and two fermion fields with different flavours, are very small.

In the Standard Model $\rho = 1$, and there are no flavour changing neutral currents. In extended models this is no longer always true.

2.1 The General Extended Higgs Model

In a general extended Higgs model the Higgs sector consists of N different multiplet fields $\Phi_k(x)$ with weak isospin T_k and hypercharge Y_k. The bosonic Lagrangian density for such a model can be obtained by generalising the Standard Model bosonic Lagrangian density (A.27) to include the Higgs fields of the extended Higgs sector:

$$\begin{aligned}\mathcal{L}_B = & -\frac{1}{4}\mathbf{W}^{\mu\nu}\cdot\mathbf{W}_{\mu\nu} - \frac{1}{4}B^{\mu\nu}B_{\mu\nu} \\ & + \sum_{k=1}^{N}(D_k{}^{\mu}\Phi_k)^{\dagger}(D_{k\mu}\Phi_k) - V(\Phi_1,...,\Phi_N) \ ,\end{aligned} \tag{2.2}$$

where the covariant derivatives are given by

$$D_k{}^{\mu} = \partial^{\mu} + ig\mathbf{T}_k\cdot\mathbf{W}^{\mu} + ig'Y_kB^{\mu} \tag{2.3}$$

and $V(\Phi_1,...,\Phi_N)$ is the generalised Higgs potential.

2.1.1 The ρ Parameter

If the vacuum state of the model is required to be invariant under the $\mathrm{U}(1)_{\mathrm{em}}$ symmetry only electrically neutral components of the Higgs fields can have non-zero vacuum expectation values. The form of the generalised Higgs potential must therefore be such that the vacuum expectation values of the Higgs fields can be written as

$$\Phi_k^{(0)}(x) = \frac{1}{\sqrt{2}}\begin{pmatrix} 0 \\ \vdots \\ 0 \\ v_k e^{i\xi_k} \\ 0 \\ \vdots \\ 0 \end{pmatrix} \quad \begin{array}{rl} T_{(3)} & = T_k \\ & \vdots \\ T_{(3)} & = -Y_k + 1 \\ T_{(3)} & = -Y_k \\ T_{(3)} & = -Y_k - 1 \\ & \vdots \\ T_{(3)} & = -T_k \end{array} \quad . \tag{2.4}$$

If the Lagrangian density (2.2) is expanded around this vacuum state the following expressions for the masses of the gauge bosons of the weak interaction are obtained:

$$m_{\mathrm{W}^\pm}^2 = \frac{g^2}{2} \sum_{k=1}^{N} v_k^2 \left(T_k(T_k+1) - Y_k^2 \right) \tag{2.5}$$

$$m_{\mathrm{Z}^0}^2 = \frac{g^2}{\cos^2\theta_{\mathrm{W}}} \sum_{k=1}^{N} v_k^2 Y_k^2 \ , \tag{2.6}$$

from which follows that [1]

$$\rho = \frac{\sum\limits_{k=1}^{N} v_k^2 \left(T_k(T_k+1) - Y_k^2 \right)}{2 \sum\limits_{k=1}^{N} v_k^2 Y_k^2} \ . \tag{2.7}$$

By choosing the vacuum expectation values carefully, the condition $\rho \approx 1$ can be fulfilled for any set of Higgs multiplet fields. This kind of arbitrary models are however considered unlikely due to the finetuning required of the vacuum expectation values in order to satisfy the constraint.

Models where $\rho = 1$ independently of the vacuum expectation values of the Higgs fields are more plausible. From the expression for ρ given above (2.7) follows that this can be achieved if the Higgs sector is restricted to contain only multiplets for which

$$T_k(T_k+1) = 3Y_k^2 \ . \tag{2.8}$$

This condition is satisfied by singlets ($T_k = 0$, $Y_k = 0$) and doublets ($T_k = \frac{1}{2}$, $Y_k = \pm\frac{1}{2}$). Other multiplets satisfying the condition, e.g. septets ($T_k = 3$, $Y_k = \pm 2$), are due to their complicated structure unlikely to be present in the theory.

For this reason the most probable extended Higgs models are those whose Higgs sector contains only singlet and doublet fields.

2.1.2 Flavour Changing Neutral Currents

If the presence of complex elements in the quark and lepton mixing matrices (A.57, A.59) is the only source of CP violation in the model, the vacuum state of the Higgs fields must be invariant under the CP

symmetry. This means that all the phases ξ_k in the vacuum expectation values (2.4) must be zero. The fermionic Lagrangian density for an extended Higgs model containing N complex Higgs doublet fields with hypercharge $Y_k = \frac{1}{2}$ can then be obtained by generalising the Standard Model fermionic Lagrangian density (A.53). The terms containing the Standard Model Higgs doublet field are repeated for each Higgs doublet field in the extended model.

$$\begin{aligned}
\mathcal{L}_F = \; & i(\bar{\Psi}^L_L \not{D} \Psi^L_L + \bar{\psi}^L_R \not{D} \psi^L_R + \bar{\psi}^N_R \not{D} \psi^N_R) \\
& + \sum_{k=1}^{N} \Big(-\bar{\Psi}^L_L G^L_k \psi^L_R \Phi_k - \Phi_k^\dagger \bar{\psi}^L_R G^L_k \Psi^L_L \\
& \qquad - \bar{\Psi}^L_L G^N_k \psi^N_R \tilde{\Phi}_k - \tilde{\Phi}_k^\dagger \bar{\psi}^N_R G^N_k \Psi^L_L \Big) \\
& + i(\bar{\Psi}^Q_L \not{D} \Psi^Q_L + \bar{\psi}^K_R \not{D} \psi^K_R + \bar{\psi}^A_R \not{D} \psi^A_R) \\
& + \sum_{k=1}^{N} \Big(-\bar{\Psi}^Q_L G^K_k \psi^K_R \Phi_k - \Phi_k^\dagger \bar{\psi}^K_R G^K_k \Psi^Q_L \\
& \qquad - \bar{\Psi}^Q_L G^A_k \psi^A_R \tilde{\Phi}_k - \tilde{\Phi}_k^\dagger \bar{\psi}^A_R G^A_k \Psi^Q_L \Big) \; . \qquad (2.9)
\end{aligned}$$

Higgs doublet fields with hypercharge $Y_k = -\frac{1}{2}$ can also be included in the model if, for these fields, the exchange $\Phi_k(x) \longleftrightarrow \tilde{\Phi}_k(x)$ is made.

From this Lagrangian density follows that the mass matrices whose diagonalisation gives the mass eigenstates of the fermion fields are

$$M^F = \sum_{k=1}^{N} \frac{v_k}{\sqrt{2}} G^F_k \quad ; \; F = L,\; N,\; K,\; A \; . \qquad (2.10)$$

The rotations in the different fermion flavour spaces that diagonalise the mass matrices M^F do not diagonalise each fermion to Higgs coupling matrix G^F_k separately. The model therefore predicts the existence of flavour changing neutral currents mediated by neutral Higgs boson fields.

A way to satisfy the experimental limits on flavour changing neutral currents is to allow all fermion fields of the same type to couple to only one of the Higgs doublet fields in the model [2]. This means that for each type of fermion field F all but one of the coupling matrices G^F_k are zero, and that the mass matrices and the remaining non-zero coupling matrices can be diagonalised simultaneously.

2.2 The Two Higgs Doublet Model

In the two Higgs doublet model (2HDM) the Higgs sector consists of two complex Higgs doublet fields with hypercharge $Y_k = \frac{1}{2}$:

$$\Phi_1(x) = \left(\begin{array}{c} \phi_1^+(x) \\ \phi_1^0(x) \end{array} \right) \ , \ \Phi_2(x) = \left(\begin{array}{c} \phi_2^+(x) \\ \phi_2^0(x) \end{array} \right) \ . \tag{2.11}$$

The most general renormalisable and gauge invariant Higgs potential is given by [3, 4]

$$\begin{aligned} V(\Phi_1, \Phi_2) = \ & \mu_1^2 {\Phi_1}^\dagger \Phi_1 + \mu_2^2 {\Phi_2}^\dagger \Phi_2 + \left(\mu_\Delta^2 {\Phi_1}^\dagger \Phi_2 + H.c. \right) \\ & + \lambda_A \left({\Phi_1}^\dagger \Phi_1 \right)^2 + \lambda_B \left({\Phi_2}^\dagger \Phi_2 \right)^2 \\ & + \lambda_C \left({\Phi_1}^\dagger \Phi_1 \right) \left({\Phi_2}^\dagger \Phi_2 \right) + \lambda_D \left({\Phi_1}^\dagger \Phi_2 \right) \left({\Phi_2}^\dagger \Phi_1 \right) \\ & + \frac{1}{2} \left(\left({\Phi_1}^\dagger \Phi_2 \right) \left(\lambda_E {\Phi_1}^\dagger \Phi_2 + \right. \right. \\ & \left. \left. \lambda_F {\Phi_1}^\dagger \Phi_1 + \lambda_G {\Phi_2}^\dagger \Phi_2 \right) + H.c. \right) \ , \end{aligned} \tag{2.12}$$

where μ_1^2, μ_2^2, λ_A, λ_B, λ_C and λ_D are real parameters while μ_Δ^2, λ_E, λ_F and λ_G may be complex. If the potential is required to be invariant under the CP symmetry, all parameters must be real.

The condition that all fermion fields of the same type couple to only one of the Higgs doublets can be enforced by requiring invariance of the Lagrangian density under the discrete symmetry

$$\Phi_1(x) \longrightarrow \Phi_1(x) \ , \ \Phi_2(x) \longrightarrow -\Phi_2(x) \tag{2.13}$$

$$\Psi_L^F(x) \longrightarrow \Psi_L^F(x) \ , \ \psi_R^F(x) \longrightarrow \pm\psi_R^F(x) \ , \tag{2.14}$$

where the plus sign applies to fermion fields that couple to $\Phi_1(x)$ and the minus sign to fermion fields that couple to $\Phi_2(x)$. If the Higgs potential is allowed to break this symmetry only 'softly', i.e. in the lowest order terms, λ_F and λ_G must be zero.

The most general renormalisable, gauge invariant and CP invariant Higgs potential can then be reparametrised as [5]

$$
\begin{aligned}
V(\Phi_1,\Phi_2) = {} & \lambda_1 \left({\Phi_1}^\dagger \Phi_1 - \frac{v_1^2}{2} \right)^2 + \lambda_2 \left({\Phi_2}^\dagger \Phi_2 - \frac{v_2^2}{2} \right)^2 \\
& + \lambda_3 \left(\left({\Phi_1}^\dagger \Phi_1 - \frac{v_1^2}{2} \right) + \left({\Phi_2}^\dagger \Phi_2 - \frac{v_2^2}{2} \right) \right)^2 \\
& + \lambda_4 \left({\Phi_1}^\dagger \Phi_1 {\Phi_2}^\dagger \Phi_2 - {\Phi_1}^\dagger \Phi_2 {\Phi_2}^\dagger \Phi_1 \right) \\
& + \lambda_5 \left(\mathrm{Re} \left({\Phi_1}^\dagger \Phi_2 \right) - \frac{v_1 v_2}{2} \right)^2 \\
& + \lambda_6 \left(\mathrm{Im} \left({\Phi_1}^\dagger \Phi_2 \right) \right)^2 \ , \qquad (2.15)
\end{aligned}
$$

where the λ's are real parameters. If all the λ's are non-negative the minimum of the potential is given for the vacuum expectation values

$$
\Phi_1^{(0)}(x) = \frac{1}{\sqrt{2}} \begin{pmatrix} 0 \\ v_1 \end{pmatrix} \ , \ \Phi_2^{(0)}(x) = \frac{1}{\sqrt{2}} \begin{pmatrix} 0 \\ v_2 \end{pmatrix} \ . \qquad (2.16)
$$

Since the sum of the squares of the two vacuum expectation values are related to the mass of the $\mathrm{W}^\pm$ boson (2.5),

$$
m_{\mathrm{W}^\pm}^2 = \frac{g^2}{4} \left(v_1^2 + v_2^2 \right) \ , \qquad (2.17)
$$

only the ratio between them are important for the predictions of the model. This ratio is usually called $\tan\beta$:

$$
\tan\beta = \frac{v_2}{v_1} \ . \qquad (2.18)
$$

Due to the Higgs mechanism three of the degrees of freedom of the Higgs fields are transformed into the longitudinal polarisation degrees of freedom of the gauge boson fields of the weak interaction. The remaining degrees of freedom correspond to physical Higgs bosons.

The Goldstone bosons, i.e. the degrees of freedom removed by the Higgs mechanism, are given by

$$
\begin{aligned}
G(x) &= \phi_1^+(x)\cos\beta + \phi_2^+(x)\sin\beta \qquad (2.19) \\
G^0(x) &= \sqrt{2} \left(\mathrm{Im}\,\phi_1^0(x)\cos\beta + \mathrm{Im}\,\phi_2^0(x)\sin\beta \right) \ . \qquad (2.20)
\end{aligned}
$$

The states orthogonal to these, i.e.

$$H(x) = -\phi_1^+(x)\sin\beta + \phi_2^+(x)\cos\beta \tag{2.21}$$

$$A^0(x) = \sqrt{2}\left(-\operatorname{Im}\phi_1^0(x)\sin\beta + \operatorname{Im}\phi_2^0(x)\cos\beta\right) , \tag{2.22}$$

correspond to a pair of charged Higgs bosons $\mathrm{H}^\pm$ and a CP-odd neutral Higgs boson A^0 with masses

$$m_{\mathrm{H}^\pm}^2 = \frac{\lambda_4}{2}(v_1^2 + v_2^2) \tag{2.23}$$

$$m_{\mathrm{A}^0}^2 = \frac{\lambda_6}{2}(v_1^2 + v_2^2) \tag{2.24}$$

The remaining degrees of freedom correspond to two CP-even neutral Higgs bosons:

$$\begin{aligned} H^0(x) &= \sqrt{2}\Big(\left(\operatorname{Re}\phi_1^0(x) - v_1\right)\cos\alpha \\ &\qquad + \left(\operatorname{Re}\phi_2^0(x) - v_2\right)\sin\alpha\Big) \end{aligned} \tag{2.25}$$

$$\begin{aligned} h^0(x) &= \sqrt{2}\Big(-\left(\operatorname{Re}\phi_1^0(x) - v_1\right)\sin\alpha \\ &\qquad + \left(\operatorname{Re}\phi_2^0(x) - v_2\right)\cos\alpha\Big) , \end{aligned} \tag{2.26}$$

where the Higgs mixing angle α and the masses can be derived by diagonalising the mass squared matrix

$$M = \begin{pmatrix} 2(\lambda_1+\lambda_3)v_1^2 + \dfrac{\lambda_5 v_2^2}{2} & \left(2\lambda_3 + \dfrac{\lambda_5}{2}\right) v_1 v_2 \\ \left(2\lambda_3 + \dfrac{\lambda_5}{2}\right) v_1 v_2 & 2(\lambda_2+\lambda_3)v_2^2 + \dfrac{\lambda_5 v_1^2}{2} \end{pmatrix} . \tag{2.27}$$

This results in

$$\tan 2\alpha = \frac{2M_{12}}{M_{11} - M_{22}} \tag{2.28}$$

and

$$m_{\mathrm{H}^0,\mathrm{h}^0}^2 = \frac{1}{2}\left(M_{11} + M_{22} \pm \sqrt{(M_{11} - M_{22})^2 + 4{M_{12}}^2}\right) . \tag{2.29}$$

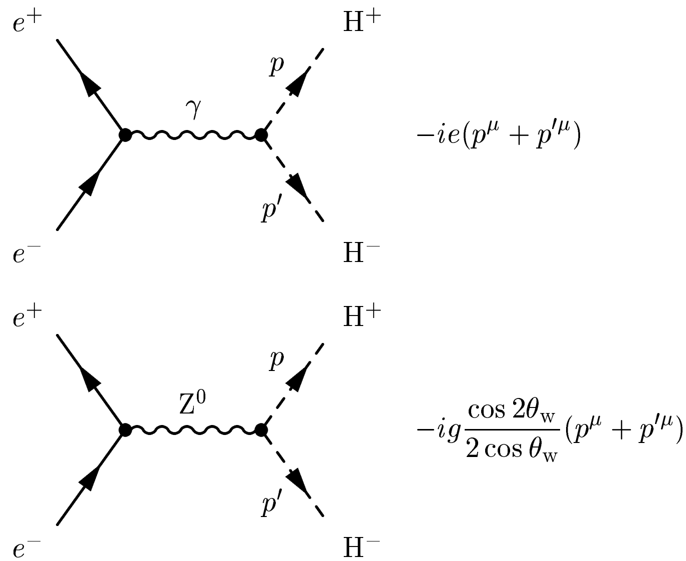

FIGURE 2.1. The Feynman diagrams describing the most important contributions to charged Higgs boson production at electron positron colliders. The vertex factors shown correspond to the $\gamma\mathrm{H}^+\mathrm{H}^-$ and $\mathrm{Z}^0\mathrm{H}^+\mathrm{H}^-$ vertices and can be derived from the 2HDM Lagrangian density.

2.2.1 Production of Charged Higgs Bosons

At an electron positron collider charged Higgs bosons are produced in pairs via an intermediate photon or Z^0 boson:

$$e^+ + e^- \longrightarrow \gamma/\mathrm{Z}^0 \longrightarrow \mathrm{H}^+ + \mathrm{H}^- \ . \tag{2.30}$$

The Feynman diagrams for these processes are shown in Figure 2.1. From these diagrams the production cross section can be calculated [6]:

$$\sigma = \frac{e^4}{48\pi s}\left(1 - \frac{4m^2_{\mathrm{H}^\pm}}{s}\right)^{\frac{3}{2}}\left(1 + \frac{2c_V c'_V}{1 - m^2_{\mathrm{Z}^0}/s} + \frac{c'^2_V(c^2_V + c^2_A)}{(1 - m^2_{\mathrm{Z}^0}/s)^2}\right) \ , \tag{2.31}$$

where

$$c_V = \frac{-1 + 4\sin^2\theta_\mathrm{w}}{4\sin\theta_\mathrm{w}\cos\theta_\mathrm{w}} \tag{2.32}$$

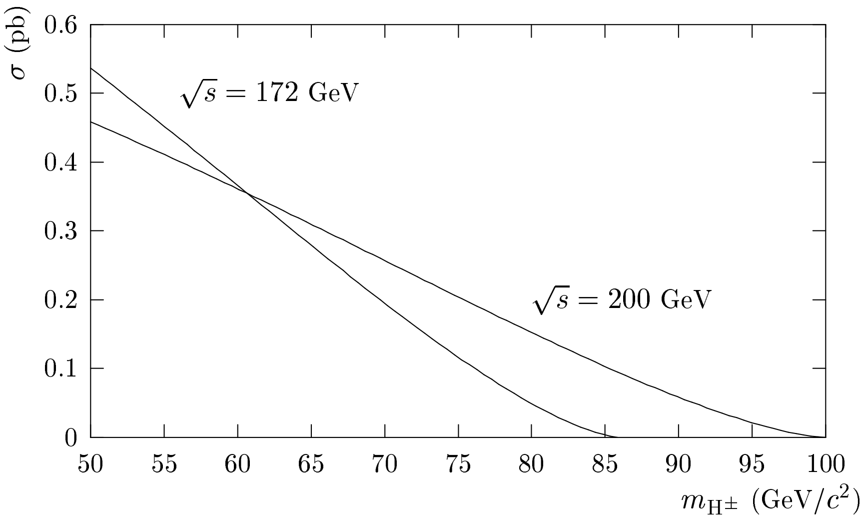

FIGURE 2.2. The tree level cross section for pair production of charged Higgs bosons ($e^{+}+e^{-} \longrightarrow \gamma/\mathrm{Z}^{0} \longrightarrow \mathrm{H}^{+}+\mathrm{H}^{-}$) as a function of the mass of the charged Higgs boson for the centre of mass energies $\sqrt{s} = 172$ GeV and $\sqrt{s} = 200$ GeV.

$$c_A = \frac{-1}{4\sin\theta_{\mathrm{w}}\cos\theta_{\mathrm{w}}} \tag{2.33}$$

$$c_V' = \frac{-1+2\sin^2\theta_{\mathrm{w}}}{2\sin\theta_{\mathrm{w}}\cos\theta_{\mathrm{w}}} \; . \tag{2.34}$$

As can be seen, the tree level cross section only depends on the centre of mass energy $\sqrt{s}$ and the charged Higgs boson mass. Figure 2.2 shows the tree level cross section as a function of the mass of the charged Higgs boson for two different centre of mass energies.

2.2.2 Decay of Charged Higgs Bosons

If the mass of the charged Higgs boson is smaller than $m_{\mathrm{W}^{\pm}} + m_{\mathrm{h}^{0}}$ and $m_{\mathrm{W}^{\pm}} + m_{\mathrm{A}^{0}}$ the decay channels $\mathrm{H}^{+} \longrightarrow \mathrm{W}^{+} + \mathrm{h}^{0}$ and $\mathrm{H}^{+} \longrightarrow \mathrm{W}^{+} + \mathrm{A}^{0}$ are not kinematically allowed. The possible decay channels are then limited to fermion channels.

The branching ratios into the different fermion channels depend on

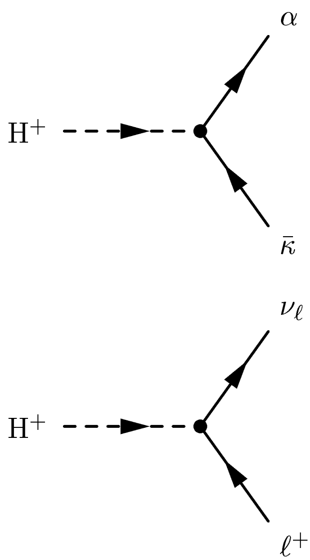

$$\frac{ig}{2\sqrt{2}m_{\mathrm{W}^\pm}} V_{\alpha\kappa}(X m_\kappa(1+\gamma_5) + Y m_\alpha(1-\gamma_5))$$

$$\frac{ig}{2\sqrt{2}m_{\mathrm{W}^\pm}} Z m_\ell(1+\gamma_5)$$

FIGURE 2.3. The Feynman diagrams describing decays of charged Higgs bosons. The corresponding vertex factors can be derived from the Lagrangian density (2.35).

the fermion to Higgs boson couplings in the Lagrangian density (2.9). For a 2HDM where each type of fermion couples to only one of the Higgs doublet fields, the terms in the Lagrangian density that describe the couplings between the fermion fields and the charged Higgs boson field can be written[1] [7]:

$$\begin{aligned}\mathcal{L}_F = \frac{g}{2\sqrt{2}m_{\mathrm{W}^\pm}} \Big(& X\bar{\psi}^A(1+\gamma_5)VM^K\psi^K H \\ & + Y\bar{\psi}^A M^A(1-\gamma_5)V\psi^K H \\ & + Z\bar{\psi}^N M^L(1+\gamma_5)\psi^L H\Big) + H.c.\ , \qquad (2.35)\end{aligned}$$

where X, Y and Z are complex numbers.

From this Lagrangian density the vertex factors for the charged Higgs fermion vertices can be derived (see Figure 2.3). From these the

[1]Here the neutrinos are considered to be massless and the Higgs couplings to the right-handed neutrino field G_k^N to be absent.

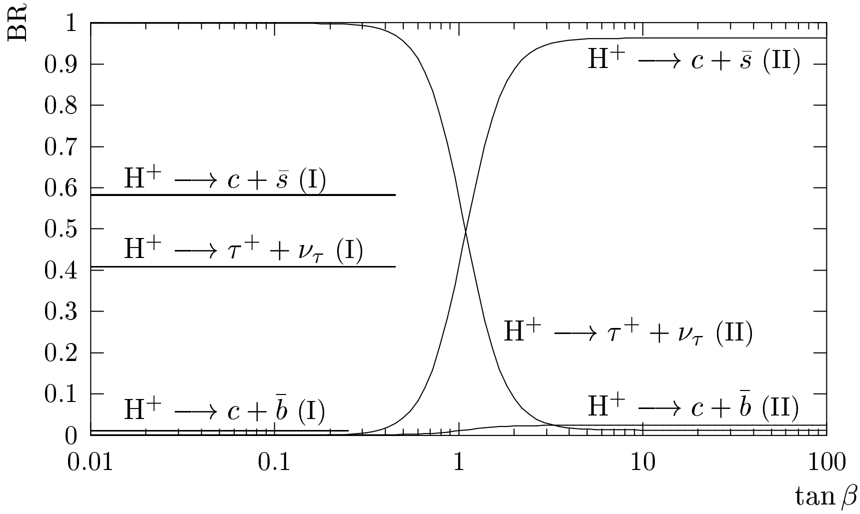

FIGURE 2.4. Branching ratios for charged Higgs bosons in two Higgs doublet models of type I and type II as a function of $\tan\beta$. In the type I model the branching ratios are independent of $\tan\beta$ and the lines have been truncated for clarity. The calculations are valid when $m_{\mathrm{H}^\pm} < m_t + m_b$, $m_{\mathrm{H}^\pm} < m_{\mathrm{W}^\pm} + m_{\mathrm{h}^0}$ and $m_{\mathrm{H}^\pm} < m_{\mathrm{W}^\pm} + m_{\mathrm{A}^0}$ so that the decay channels $\mathrm{H}^+ \longrightarrow t+\bar{b}$, $\mathrm{H}^+ \longrightarrow \mathrm{W}^+ + \mathrm{h}^0$ and $\mathrm{H}^+ \longrightarrow \mathrm{W}^+ + \mathrm{A}^0$ are kinematically forbidden. The small branching ratio for $\mathrm{H}^+ \longrightarrow c+\bar{b}$ is due to the small value of the $|V_{cb}|$ matrix element. Particle masses and CKM matrix elements used in the calculations have been taken from the Review of Particle Physic [8]. Since quarks have non-zero colour charges they are never found as free particles. For this reason the mass of a free quark is not a well defined quantity, and some sort of estimate must be used. In the calculations the central values of the estimated mass ranges in the Review have been used.

partial decay widths can be calculated:

$$\Gamma(\mathrm{H}^+ \longrightarrow \alpha + \bar{\kappa}) = N_c \, \frac{g^2 m_{\mathrm{H}^\pm}}{32\pi m_{\mathrm{W}^\pm}^2} \, |V_{\alpha\kappa}|^2 (|X|^2 m_\kappa^2 + |Y|^2 m_\alpha^2) \tag{2.36}$$

$$\Gamma(\mathrm{H}^+ \longrightarrow \ell^+ + \nu_\ell) = \frac{g^2 m_{\mathrm{H}^\pm}}{32\pi m_{\mathrm{W}^\pm}^2} \, |Z|^2 m_\ell^2 \ , \tag{2.37}$$

where $N_c = 3$ is the number of colours.

The different versions of the 2HDM are classified according to which fermion fields couple to which Higgs doublet field. In the so called type I model all fermions couple to the same Higgs doublet, resulting in

$$X = Z = -\cot\beta \ , \ Y = \cot\beta \ . \tag{2.38}$$

In this model the branching ratios are independent of $\tan\beta$.

In the so called type II model up-type quarks couple to one Higgs doublet and down-type quarks and charged leptons couple to the other, resulting in

$$X = Z = \tan\beta \ , \ Y = \cot\beta \ . \tag{2.39}$$

The branching ratio as a function of $\tan\beta$ can be found for the two models in Figure 2.4. As can be seen from this figure the two decay channels $\mathrm{H}^+ \longrightarrow \tau + \nu_\tau$ and $\mathrm{H}^+ \longrightarrow c + \bar{s}$ together adds up to almost 100% of the decays. The ratio between them is however model dependent. A model independent search for pair produced charged Higgs boson must therefore search for three different final states: a hadronic final state ($c\bar{s}\bar{c}s$) if both charged Higgs bosons decay into quarks, a semileptonic final state ($c\bar{s}\tau^-\bar{\nu}_\tau$ or $\tau^+\nu_\tau\bar{c}s$) if one of the charged Higgs bosons decays into quarks and the other into leptons and a leptonic final state ($\tau^+\nu_\tau\tau^-\bar{\nu}_\tau$) if both charged Higgs bosons decay into leptons.

2.3 The Minimal Supersymmetric Model

Supersymmetry (SUSY) predicts that every particle has a supersymmetric partner. The supersymmetric partner of a fermion is a boson, and the partner of a boson is a fermion. All quantum numbers, except the spin, are the same for the particle and its partner.

If supersymmetry would be an exact symmetry also the masses of the particle and its supersymmetric partner would be equal. However, no supersymmetric partners to the known particles have been observed. The supersymmetric partners are therefore assumed to be heavy enough not to have been observed experimentally. This means that supersymmetry must be a broken symmetry so that there exist terms in the Lagrangian density of the model that are not invariant under the supersymmetric transformation where the particle fields are replaced by the fields of their supersymmetric partners.

One of the motivations for supersymmetric models is that the large corrections to the mass of the Higgs boson that arise in the Standard Model due to fermion loops when using perturbation theory beyond the tree level can be cancelled by contributions from loops containing the supersymmetric partners of the fermions.

Another motivation is that supersymmetry is an essential part of a number of theories that try to incorporate gravity into the Standard Model.

In a supersymmetric model a Higgs doublet field $\Phi(x)$ and its conjugate field $\tilde{\Phi}(x)$ can not both be present in the Lagrangian density. The up-type and down-type quarks can therefore not couple to the same Higgs doublet field, which means that the Minimal Supersymmetric Model (MSSM) must be a two Higgs doublet model of type II.

Supersymmetry imposes constraints on the λ parameters in the Higgs potential of the 2HDM (2.15). These constraints can be summarised as follows [9]:

$$\lambda_2 = \lambda_1 \tag{2.40}$$

$$\lambda_3 = \frac{1}{8}(g^2 + g'^2) - \lambda_1 \tag{2.41}$$

$$\lambda_4 = 2\lambda_1 - \frac{1}{2}g'^2 \tag{2.42}$$

$$\lambda_5 = \lambda_6 = 2\lambda_1 - \frac{1}{2}(g^2 + g'^2) \ . \tag{2.43}$$

When these constraints are inserted into the expressions for the Higgs boson masses (2.23, 2.24, 2.29) the following relations between the masses are obtained:

$$m_{\mathrm{H}^\pm}^2 = m_{\mathrm{A}^0}^2 + m_{\mathrm{W}^\pm}^2 \tag{2.44}$$

$$m_{\mathrm{H}^0,\mathrm{h}^0}^2 = \frac{1}{2}\left(m_{\mathrm{A}^0}^2 + m_{\mathrm{Z}^0}^2 \pm \sqrt{(m_{\mathrm{A}^0}^2 + m_{\mathrm{Z}^0}^2)^2 - 4m_{\mathrm{A}^0}^2 m_{\mathrm{Z}^0}^2 \cos^2 2\beta}\right) \ , \tag{2.45}$$

and the Higgs mixing angle α (2.28) can be written as:

$$\tan 2\alpha = \tan 2\beta \left(\frac{m_{\mathrm{H}^0}^2 + m_{\mathrm{h}^0}^2}{m_{\mathrm{A}^0}^2 - m_{\mathrm{Z}^0}^2}\right) \ . \tag{2.46}$$

As can be seen from the mass relations above the mass spectrum of the Higgs bosons in the MSSM can be parametrised in terms of m_{A^0} and $\tan\beta$.

CHAPTER 3

LEP and DELPHI

In the Large Electron Positron (LEP) collider at the European laboratory for particle physics (CERN) in Geneva, Switzerland, beams of electrons and positrons are accelerated in opposite directions. The beams collide with each other at four different points, where large experimental facilities have been built in order to register the outcome of the collisions. These detectors are called ALEPH, DELPHI, L3 and OPAL. The analysis described in this thesis has been performed using data collected by the DELPHI detector.

3.1 LEP

The Large Electron Positron collider is a storage ring located in a 27 km long tunnel 100 m below ground level on the border between Switzerland and France. The construction of the collider began in 1983 and it was put into operation in 1989. After twelve years of successful running it was finally closed down in November 2000.

During the so called LEP 1 period, which lasted until October 1995, the electron and positron beams were collided at a centre of mass energy close to the mass of the Z^0 boson. In these collisions several million Z^0 bosons were produced, and their decays were studied with the help of the four detectors.

In November 1995 the LEP 2 period began. During this period the centre of mass energy of the collisions was gradually increased. In 1996 the centre of mass energy reached 161 GeV, which made pair production of $W^{\pm}$ bosons via an intermediate photon or Z^0 boson ($e^+ + e^- \longrightarrow$

TABLE 3.1. The centre of mass energies ($\sqrt{s}$) at which data were collected during the LEP 2 period, and the amount of data collected (integrated luminosity) by the DELPHI detector at the different centre of mass energies. During 2000 the collider was not run at a fixed centre of mass energy, but was run at the highest possible energy depending on the state of the collider. This resulted in a distribution of centre of mass energies in the range 200–208 GeV.

Year	$\sqrt{s}$	$\int \mathcal{L}dt$
1995	130 GeV	3 pb^{-1}
	136 GeV	3 pb^{-1}
1996	161 GeV	10 pb^{-1}
	172 GeV	10 pb^{-1}
1997	183 GeV	55 pb^{-1}
1998	189 GeV	158 pb^{-1}
1999	192 GeV	26 pb^{-1}
	196 GeV	77 pb^{-1}
	200 GeV	84 pb^{-1}
	202 GeV	41 pb^{-1}
2000	200–208 GeV	225 pb^{-1}

$\gamma/\mathrm{Z}^0/ \longrightarrow \mathrm{W}^+ + \mathrm{W}^-$) kinematically possible. During the last year of running the collider reached a centre of mass energy of 208 GeV. Table 3.1 lists the centre of mass energies at which data were collected during the LEP 2 period. It also lists the amount of data (integrated luminosity) that was collected by the DELPHI detector at the different centre of mass energies.

3.2 DELPHI

The Detector with Lepton, Photon and Hadron Identification (DELPHI) was designed to be a general purpose detector. It has been used for a large variety of studies, ranging from precision measurements of the parameters of the Standard Model to searches for new particles.

The DELPHI detector and its performance have been described in detail in several publications [10, 11] and only a short description will be given here. The detector has the shape of a cylinder with a radius of 6 m and a length of 10 m. It consists of a central part, called the barrel, and two end-caps. The layout of the barrel and one of the end-caps is shown in Figure 3.1.

The DELPHI detector consists of several subdetectors that have been designed to perform different tasks. The different subdetectors can be divided into three main categories depending on their primary function.

3.2.1 Tracking

The first category is the tracking detectors. These register ionisations caused by charged particles traversing the detector medium. From these registered hits the tracks of the particles can be reconstructed.

The superconducting coil surrounding the tracking detectors provides a magnetic field that causes the charged particle tracks to bend. By measuring the curvature of a track information about the momentum and the charge of the particle can be obtained.

The tracking detector closest to the interaction point is called the Vertex Detector. This detector can be used to reconstruct secondary decay vertices. Other tracking detectors are the Inner and Outer Detectors, the Time Projection Chamber and the Forward Chambers A and B.

3.2.2 Calorimetry

The second category of subdetectors is the calorimeters. These measure the total energy of the particles by collecting the total energy deposited in the detector when the particles shower, slow down and stop.

The DELPHI detector has many calorimeters. Among them the High Density Projection Chamber and the Forward Electromagnetic Calorimeter are mainly intended for measuring the energy of electrons and photons, while the Barrel and Forward Hadron Calorimeters are intended for measuring the energy of hadrons.

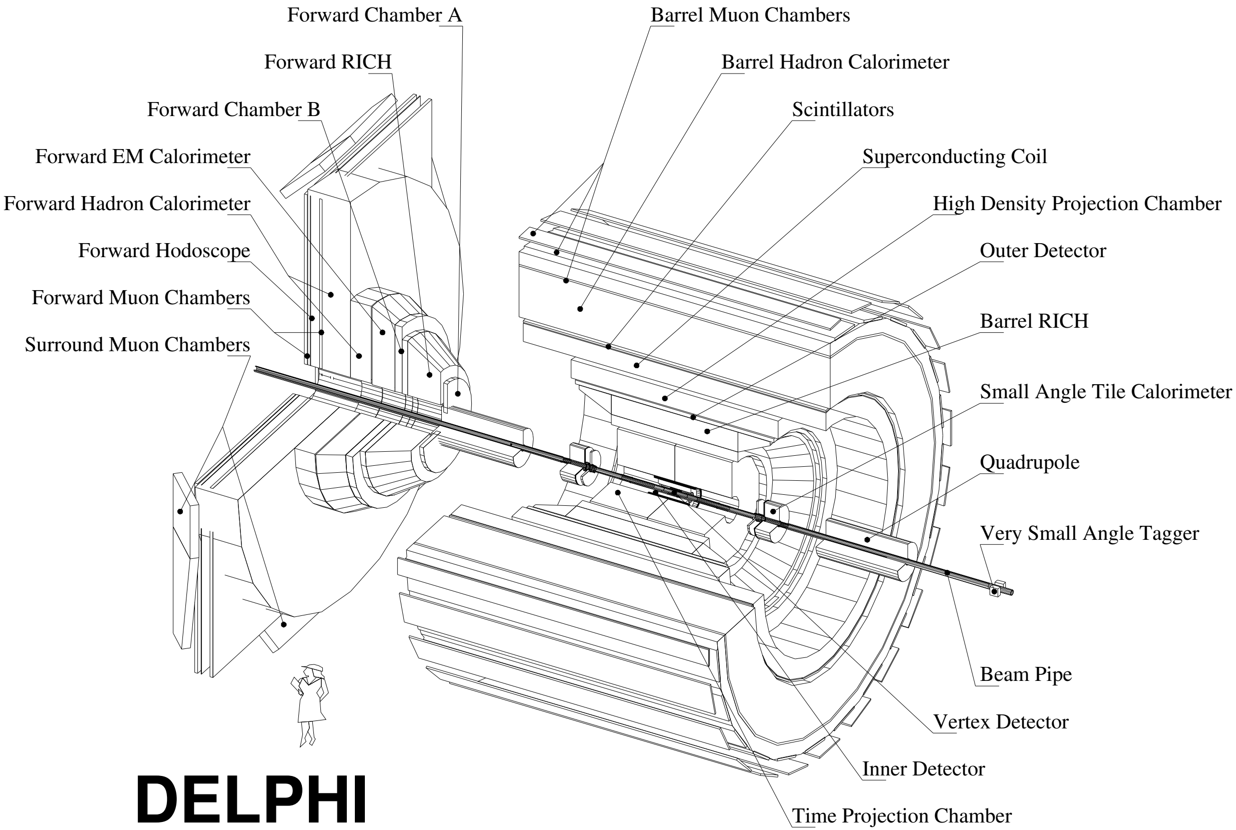

FIGURE 3.1. The DELPHI detector

3.2.3 Particle Identification

The third category of subdetectors is dedicated to identifying what kind of particles are passing through the detector. The DELPHI detector was designed to provide good particle identification over a large momentum range.

The information obtained from measuring the energy loss ($-dE/dx$) in the tracking detectors can be used to identify charged particles with low momenta, and electrons and photons can be identified using information from the calorimeters.

There are also special subdetectors dedicated to particle identification. The Muon Chambers are the outermost subdetectors. These can identify muons, since muons are the only charged particles that are not stopped in the calorimeters.

The Barrel and Forward Ring Imaging Cherenkov (RICH) detectors detect photons radiated by charged particles that pass through a medium at a speed faster than the speed of light in that medium. The angle of emission (Cherenkov angle) depends of the refractive index of the medium and the speed of the particle. By combining the measurement of the Cherenkov angle with the momentum measurement from the tracking detectors the particle can be identified. In order to provide particle identification over a large momentum range the RICH detectors consist of two parts containing different media (one liquid and one gas) with different refractive indices. The RICH detectors provide separation between pions, kaons and protons over the full momentum range 1–20 GeV/c (see Figure 3.2).

The Uppsala DELPHI group contributed to the invention of these detectors and took an active role in their construction in the 1980's. Among the four LEP experiments, only DELPHI was provided with RICH detectors.

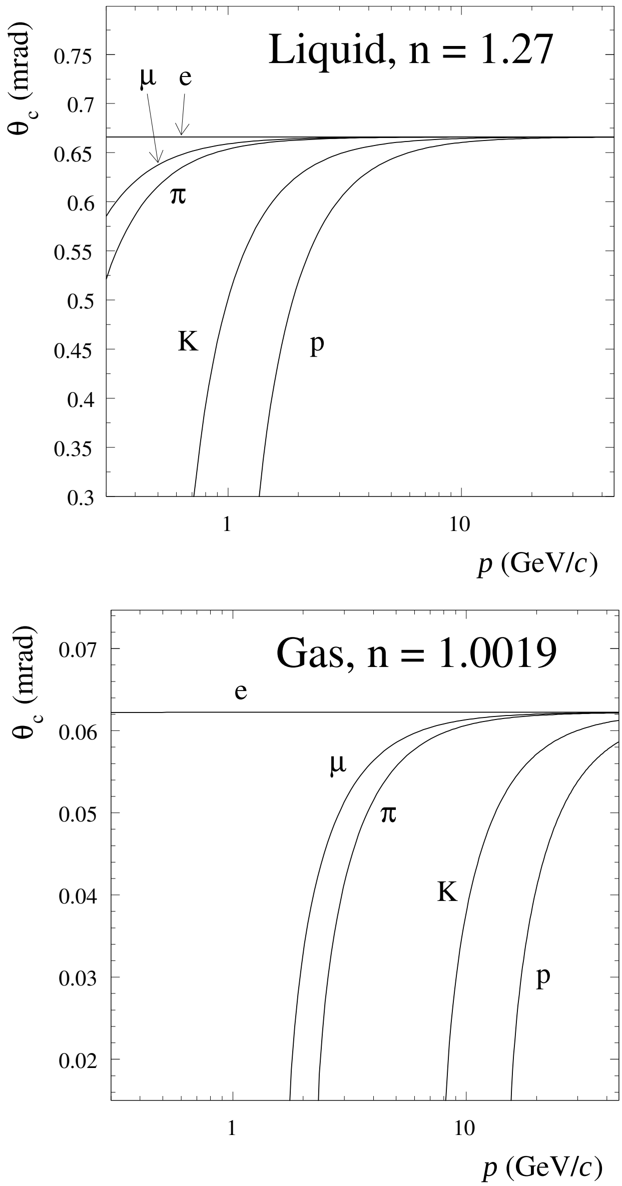

FIGURE 3.2. The Cherenkov angle as a function of momentum for different particles in the liquid and gas RICH detectors in the DELPHI detector.

CHAPTER 4

Analysis

The data set collected by the DELPHI detector consists of several million events. From these events, those compatible with a signal originating from the pair production of charged Higgs bosons must be selected. The background, from which this signal must be separated, consists of events originating from the known processes of the Standard Model: Bhabha scattering, production of fermion-antifermion pairs, pair production of $W^{\pm}$ bosons and so on.

With the help of Monte Carlo simulated samples of signal and background events a set of criteria can be designed to select signal events with a high efficiency, while rejecting a large fraction of the background events.

Some components of the background can easily be rejected by applying cuts on single variables without reducing the efficiency for selecting signal events significantly. Examples of this kind of cuts are the requirements that at least eight charged particle tracks are reconstructed in the event, or that the sum of the energies of the particles observed in the event exceeds 30% of the available centre of mass energy.

Other components of the background behave very similarly to the signal. In the search for a signal originating from the pair production of charged Higgs bosons, this is particularly true for the background originating from the pair production of $W^{\pm}$ bosons. This kind of background can not be rejected by simple cuts on single variables without seriously decreasing the signal detecting efficiency.

In order to discriminate between the charged Higgs boson signal and the $W^{\pm}$ boson background the differences between the two kinds of events must be used. Since the charged Higgs boson has spin 0 and the $W^{\pm}$ boson has spin 1 the two processes have different differential production cross sections. The spin difference also gives rise to differences in the distribution of the decay angles of the produced bosons, and in the polarisation of the tauons created in their decays [12].

4.1 Combining Information

Background events can be rejected more efficiently when information from many variables are combined into a discriminating variable on which the selection cut is made. In the analysis two different methods have been used to construct this discriminating variable.

4.1.1 Fisher Discriminant

A Fisher discriminant [13] is a weighted sum of a number of variables x_i describing the event:

$$F = \sum_{i=1}^{N} \lambda_i x_i \ . \tag{4.1}$$

With the help of Monte Carlo simulated samples of signal and background events, the weights λ_i are derived in order to maximise the separation S between signal and background events:

$$S = \frac{\langle F \rangle_{\mathrm{s}} - \langle F \rangle_{\mathrm{b}}}{(\sigma_F^2)_{\mathrm{s}} + (\sigma_F^2)_{\mathrm{b}}} \ . \tag{4.2}$$

4.1.2 Likelihood Functions

This method uses the normalised distributions of the observed variables for signal $f_i^{\mathrm{s}}(x_i)$ and background $f_i^{\mathrm{b}}(x_i)$ events obtained from Monte Carlo simulated samples to define the probability ratio for a measured value x_i to be compatible with signal or background:

$$P_i^{\mathrm{s}}(x_i) = \frac{f_i^{\mathrm{s}}(x_i)}{f_i^{\mathrm{s}}(x_i) + f_i^{\mathrm{b}}(x_i)} \tag{4.3}$$

$$P_i^{\mathrm{b}}(x_i) = \frac{f_i^{\mathrm{b}}(x_i)}{f_i^{\mathrm{s}}(x_i) + f_i^{\mathrm{b}}(x_i)} \ . \tag{4.4}$$

These probability ratios are then combined to form a combined likelihood function $\mathcal{L}$ for the event to be compatible with the signal:

$$\mathcal{L} = \frac{\prod_{i=1}^{N} P_i^{\mathrm{s}}(x_i)}{\prod_{i=1}^{N} P_i^{\mathrm{s}}(x_i) + \prod_{i=1}^{N} P_i^{\mathrm{b}}(x_i)} . \tag{4.5}$$

4.2 Quark Flavour Tagging

The decay branching fractions are different for the charged Higgs bosons and the $W^{\pm}$ bosons. A charged Higgs boson decaying into quarks creates a cs quark pair, while a $W^{\pm}$ boson decaying into quarks creates either a cs or a ud quark pair. If the flavour of the quarks can be tagged and events containing cs quark pairs can be selected, the part of the $W^{\pm}$ boson background decaying into ud quark pairs can be suppressed.

4.2.1 Charged Kaons and Quark Flavour Confidence

The first attempt to tag c and s quarks was made in the analysis of the data collected at $\sqrt{s} = 172$ GeV. This method used the fact that the number of kaons with high momenta is expected to be greater in jets coming form c and s quarks than in jets coming from u and d quarks. For this reason the variable

$$f_{\mathrm{K}} = \frac{1}{\sqrt{s}} \sum_i p_i \tag{4.6}$$

was constructed, where p_i is the momentum of particle i and the the sum was taken over all particles i identified by the RICH detectors as being charged kaons.

In order to select events containing c quarks, the so called c quark confidence was used [14]. This variable combines information about every track in the event to derive a likelihood that the tracks in the event belong to a c quark jet. For each track the information used is its impact parameter significance and its momentum, and the angle between the track and the axis of the jet the track belongs to.

4.2.2 The Jet Flavour Tagging Algorithm

Later a jet flavour tagging algorithm developed within the DELPHI collaboration was used [15]. This algorithm combines several pieces of information about a jet in order to tag the flavour of the quark from which the jet originated. The variables used in the algorithm are

- the fraction of charged jet energy,
- the fraction of the charged jet energy that comes from identified kaons and protons,
- the energy of the leading particle in the jet,
- the number of identified leptons in the jet,
- the b quark confidence (calculated using the tracks in the jet),
- the c quark confidence (calculated using the tracks in the jet),
- the scaled invariant mass of the secondary particle in the jet,
- the compatibility with the primary vertex of the first track yielding a secondary vertex mass above the D meson mass when the tracks are sorted in decreasing order of b probability, and
- the minimum pion momentum transverse to the jet axis (this variable was designed to be sensitive to pions with low transverse momenta produced in the decay of D^* mesons).

The variables are combined into a likelihood function. The likelihoods for the individual jets to have originated from a c or s quark have been combined into an event cs tag (for the semileptonic channel) or an event $cscs$ tag (for the hadronic channel).

4.3 Limit Derivation

No excess with respect to the expected number of events from the background has been observed in the analysis. The result has therefore been used to derive an exclusion limit. Two different methods to calculate the confidence level for the exclusion have been used.

4.3.1 Bayesian Approach

In the Bayesian approach the probability for the presence of a signal with an expected number of events s' that is greater than the expected number of events from the signal hypothesis s is calculated, given the outcome of n observed events in the experiment [16].

$$P(s' > s|n) = \int_s^\infty f(s'|n)ds' \tag{4.7}$$

With the help of Bayes' theorem this expression is written in terms of the known probabilities $P(n|s')$.

$$f(s'|n) = \frac{P(n|s')f(s')}{P(n)} = \frac{P(n|s')f(s')}{\int_0^\infty P(n|s')f(s')ds'} \tag{4.8}$$

All s' are assumed to have the same à priori probability, i.e. $f(s') =$ const. From this assumption follows that

$$f(s'|n) = \frac{P(n|s')}{\int_0^\infty P(n|s')ds'} \ . \tag{4.9}$$

Equation (4.9) inserted in (4.7) gives

$$P(s' > s|n) = \frac{\int_s^\infty P(n|s')ds'}{\int_0^\infty P(n|s')ds'} \ . \tag{4.10}$$

The signal hypothesis is said to be excluded at a confidence level of CL if

$$1 - P(s' > s|n) = 1 - \frac{\int_s^\infty P(n|s')ds'}{\int_0^\infty P(n|s')ds'} \geq CL \ . \tag{4.11}$$

The number of events observed in a single channel experiment is Poisson distributed. The probability to observe n events in an experiment with an expected background of b events and an expected signal of s' events is

$$P(n|s') = \frac{e^{-(s'+b)}(s'+b)^n}{n!} \ . \tag{4.12}$$

This probability inserted in (4.11) results in an exclusion of the signal at a confidence level of CL if

$$1 - e^{-s}\frac{\sum_{k=0}^{n}\frac{(s+b)^k}{k!}}{\sum_{k=0}^{n}\frac{b^k}{k!}} \geq CL \ . \tag{4.13}$$

The method to derive the confidence level in a single channel experiment described above can be generalised to a multichannel experiment. In an experiment with N channels the probability to see n events if there exists a signal with an expected number of events s' is

$$P(n|s') = \prod_{i=1}^{N} \frac{e^{-(s'p_i+b_i)}(s'p_i + b_i)^{n_i}}{n_i!} \ , \tag{4.14}$$

where n_i is the number of observed events in channel i, b_i and s_i are the expected number of events in channel i from background and signal events respectively and

$$p_i = \frac{s_i}{\sum_{i=1}^{N} s_i} \tag{4.15}$$

is the fraction of the total number of expected signal events that is expected in channel i.

This probability inserted in (4.11) results in an exclusion of the signal at a confidence level of CL if

$$1 - e^{-s} \frac{\prod_{i=1}^{N} \sum_{k=0}^{n_i} \frac{(s + b_i/p_i)^k}{k!}}{\prod_{i=1}^{N} \sum_{k=0}^{n_i} \frac{(b_i/p_i)^k}{k!}} \geq CL \ . \tag{4.16}$$

When combining results from different centre of mass energies, each final state at each centre of mass energy has been treated as a separate channel.

4.3.2 A Likelihood Ratio Monte Carlo (ALRMC)

The ALRMC method [17] uses a likelihood ratio Q to order the possible outcomes of an experiment in increasingly signal-like order. In a search experiment the likelihood ratio used is the ratio of the likelihoods for the signal+background and background-only hypotheses:

$$Q = \frac{\mathcal{L}(s + b)}{\mathcal{L}(b)} \ . \tag{4.17}$$

The confidence in the signal+background hypothesis is given by the probability that Q is less than or equal to the value observed in an experiment under the assumption that the signal+background hypothesis is true:

$$CL_{\mathrm{s+b}} = P(Q \leq Q_{\mathrm{obs}}|\mathrm{s+b}) = \int_0^{Q_{\mathrm{obs}}} f(Q'|\mathrm{s+b})dQ' \; . \tag{4.18}$$

Similarly the confidence in the background only hypothesis is defined as the probability that Q is less than or equal to the value observed under the assumption that the background only hypothesis is true:

$$CL_{\mathrm{b}} = P(Q \leq Q_{\mathrm{obs}}|\mathrm{b}) = \int_0^{Q_{\mathrm{obs}}} f(Q'|\mathrm{b})dQ' \; . \tag{4.19}$$

The signal hypothesis is said to be excluded at a confidence level of CL if

$$1 - CL_{\mathrm{s}} = 1 - \frac{CL_{\mathrm{s+b}}}{CL_{\mathrm{b}}} \geq CL \; . \tag{4.20}$$

The likelihood ratio for an experiment with N channels is given by

$$\begin{aligned} Q &= \frac{\displaystyle\prod_{i=1}^{N} \frac{e^{-(s_i+b_i)}(s_i+b_i)^{n_i}}{n_i!} \prod_{j=1}^{n_i} \frac{s_i f_i^{\mathrm{s}}(x_i^{(j)}) + b_i f_i^{\mathrm{b}}(x_i^{(j)})}{s_i+b_i}}{\displaystyle\prod_{i=1}^{N} \frac{e^{-b_i} b_i^{n_i}}{n_i!} \prod_{j=1}^{n_i} f_i^{\mathrm{b}}(x_i^{(j)})} \\ &= e^{-s} \prod_{i=1}^{N} \prod_{j=1}^{n_i} \left(1 + \frac{s_i f_i^{\mathrm{s}}(x_i^{(j)})}{b_i f_i^{\mathrm{b}}(x_i^{(j)})} \right) \; , \end{aligned} \tag{4.21}$$

where $f_i^{\mathrm{s}}(x_i)$ and $f_i^{\mathrm{b}}(x_i)$ are probability density functions for some discriminating variable x_i for signal and background events respectively. For the hadronic and semileptonic final states where the mass of the charged Higgs boson can be reconstructed, the reconstructed mass can be used as a discriminating variable, i.e. $f(x) = f(m_{\mathrm{H}^\pm}^{\mathrm{rec}})$. Otherwise, any variable that separates signal and background can be used, e.g. a likelihood function: $f(x) = f(\mathcal{L})$. In order to take more information about the events into account two-dimensional probability density functions can be used, e.g. $f(x) = f(m_{\mathrm{H}^\pm}^{\mathrm{rec}},\ \mathcal{L})$.

The probability density functions for Q used to define the confidences $CL_{\mathrm{s+b}}$ and CL_{b} can in the general case not be derived analytically. They are therefore obtained using Monte Carlo sampling from the distributions of the discriminating variables for signal and background events.

For a single channel simple counting experiment ($N = 1$, $f^{\mathrm{s}}(x) = f^{\mathrm{b}}(x) = 1$) the likelihood ratio is

$$Q = e^{-s}\left(1 + \frac{s}{b}\right)^n \ , \tag{4.22}$$

from which follows that

$$P(Q \le Q_{\mathrm{obs}}) = P(n \le n_{\mathrm{obs}}) \ . \tag{4.23}$$

For a counting experiment the number of candidates is Poisson distributed:

$$P(n \le n_{\mathrm{obs}}|\mathrm{s+b}) = \sum_{n=0}^{n_{\mathrm{obs}}} \frac{e^{-(s+b)}(s+b)^n}{n!} \tag{4.24}$$

$$P(n \le n_{\mathrm{obs}}|\mathrm{b}) = \sum_{n=0}^{n_{\mathrm{obs}}} \frac{e^{-b}b^n}{n!} \ , \tag{4.25}$$

which results in an exclusion of the signal hypothesis at a confidence level of CL if

$$1 - e^{-s}\frac{\displaystyle\sum_{n=0}^{n_{\mathrm{obs}}} \frac{(s+b)^n}{n!}}{\displaystyle\sum_{n=0}^{n_{\mathrm{obs}}} \frac{b^n}{n!}} \le CL \ , \tag{4.26}$$

a result that agrees with the result obtained for a single channel experiment using the Bayesian approach (4.13). For a single channel simple counting experiment the two methods give the same result.

CHAPTER 5

Summary

The first results from the search for charged Higgs bosons published by the DELPHI collaboration used data collected during the LEP 1 period. Later, during the LEP 2 period, when the centre of mass energy of the collisions was increased, new results were published almost every year.

5.1 LEP 1

The search for charged Higgs bosons using the data collected during the LEP 1 period [18] considered only two of the three possible final states. The hadronic final state was analysed using data collected by the DELPHI detector in 1991, 1992 and 1993 and the leptonic final state was analysed using data collected in 1990 and 1991. No evidence for the existence of charged Higgs bosons was found. A statistical analysis of the result excluded the existence of a charged Higgs boson with a mass lower than 43.5 GeV/c^2 at 95% confidence level independently of the decay branching ratios of the charged Higgs boson (see region A in Figure 5.1).

5.2 $\sqrt{s} = 130$–136 GeV

The data collected in November 1995 at $\sqrt{s} = 130$–136 GeV were analysed in order to search for charged Higgs bosons in the hadronic final state [19]. After a set of cuts selecting four-jet events, a Fisher discriminant analysis (see section 4.1.1) was used to reject the remaining background. No significant indication of existence of charged Higgs bosons was observed. Due to the small size of the collected data sample the analysis was not able to exclude the existence of charged Higgs bosons at 95% confidence level anywhere outside the region already excluded by the LEP 1 result.

5.3 $\sqrt{s} = 161$ GeV

The data collected in the Summer of 1996 at $\sqrt{s} = 161$ GeV were analysed in order to search for charged Higgs bosons in all three final states [20]. The data collected the previous year at $\sqrt{s} = 130$ and 136 GeV were reanalysed using a similar method. No significant excess compatible with a signal from a charged Higgs boson was found. When combining the results from the three centre of mass energies the existence of a charged Higgs boson was excluded at 95% confidence level for masses below 51.5 GeV/c^2 for leptonic branching ratios of the charged Higgs boson above 0.2 (see region B in Figure 5.1).

After the analysis of the $\sqrt{s} = 161$ GeV data Rémi Silvestre, who had been responsible for the charged Higgs boson search within the DELPHI collaboration during the LEP 2 period, presented his Ph.D. thesis [21] and left the collaboration.

5.4 $\sqrt{s} = 172$ GeV (Paper I)

My Ph.D. studies began during the Summer of 1996 and I started working on the charged Higgs boson analysis within the DELPHI collaboration later that year. My first responsibility was to analyse the data collected at $\sqrt{s} = 172$ GeV during the second half of 1996. This analysis, presented in paper I [22], is very similar to the earlier analysis of the $\sqrt{s} = 161$ data. However, since the centre of mass energy now was well above the threshold for production of $W^{\pm}$ pairs, the composition of the background that must be rejected by the analysis had changed from being mainly $q\bar{q}$ to an increasingly more important contribution from $W^{\pm}$ pairs. For this reason additional variables used for cs quark tagging (see section 4.2.1) were introduced in the Fisher discriminants in the analysis. When combined with the earlier results the new analysis excluded the existence of a charged Higgs boson with a mass lower than

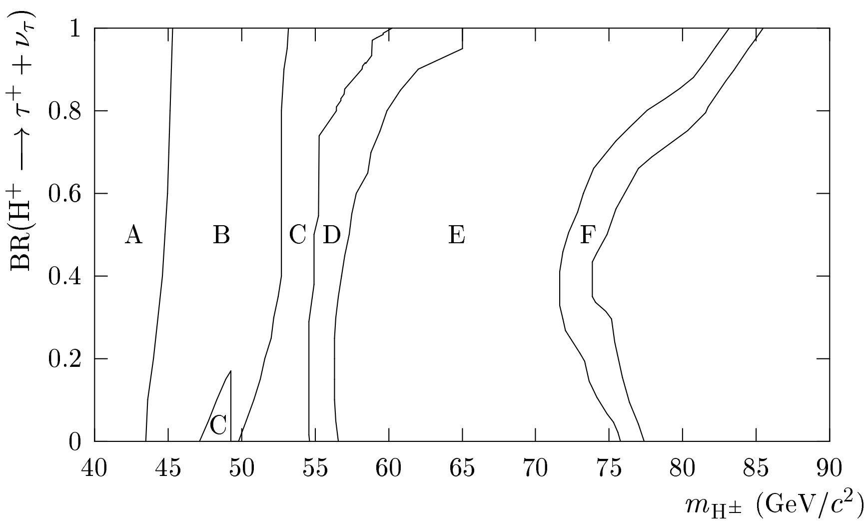

FIGURE 5.1. The regions in the parameter space spanned by $m_{H^\pm}$ and BR($H^+ \longrightarrow \tau^+ + \nu_\tau$) that have been excluded at 95% confidence level using the data collected by the DELPHI detector at (A) LEP 1 [18], (B) $\sqrt{s} = 130$, 136 and 161 GeV [20], (C) $\sqrt{s} = 130$, 136, 161 and 172 GeV [22], (D) $\sqrt{s} = 161$, 172 and 183 GeV [23], (E) $\sqrt{s} = 189$–202 GeV [24] and (F) $\sqrt{s} = 189$–208 GeV [25].

54.5 GeV/c^2 at 95% confidence level independently of the branching ratios of charged Higgs boson (see region C in Figure 5.1).

5.5 $\sqrt{s} = 183$ GeV (Paper II)

By the time the data collected in 1997 at $\sqrt{s} = 183$ GeV were analysed more people had joined the charged Higgs boson search in the DELPHI collaboration. In the analysis presented in paper II [23] I was responsible for the semileptonic and leptonic final states.

In the new analysis the discriminating variables were constructed as likelihood functions (see section 4.1.2) instead of Fisher discriminants. The new analysis also made use of the new jet flavour tagging (see section 4.2.2) and the new limit calculation method (see section 4.3.2). The data collected at $\sqrt{s} = 161$ and 172 GeV were reanalysed using the improved method and the results from the three centre of mass energies were combined. No significant excess was found and a 95% confidence level exclusion limit for the existence of charged Higgs bosons was set at 56.3 GeV/c^2 independently of the branching ratios of the charged Higgs boson (see region D in Figure 5.1).

5.6 $\sqrt{s}$ = 189–202 GeV (Paper III)

In 1998 the centre of mass energy of the collisions was 189 GeV and in 1999 it was gradually increased, and data were collected at $\sqrt{s} = 192$, 196, 200 and 202 GeV. When these data were analysed the group in the DELPHI collaboration responsible for the charged Higgs boson search had grown even more. In the analysis presented in paper III [24] I was responsible for the semileptonic final state.

The analysis method was similar to the one used for the $\sqrt{s} = 183$ GeV data. Some enhancements in the selection of tauons was made by identifying their decay products and estimating their polarisation. The limit calculation was improved by using two-dimensional distributions in the calculation of the likelihood ratios. No signal like excess was found and the charged Higgs boson mass limit was set at 71.5 GeV/c^2 at 95% confidence level independently of the branching ratios of the charged Higgs boson (see region E in Figure 5.1). The large increase in the exclusion limit with respect to the previous analysis is due to the large increase in integrated luminosity.

5.7 $\sqrt{s}$ up to 208 GeV (Papers IV and V)

The analysis of the data collected during 2000 is still preliminary since not all energy calibrations and detector efficiencies have been accounted for. The analysis is the same as the one used for the $\sqrt{s}$ = 189–202 GeV data. The analysis presented in paper IV [26] uses the first 74 pb^{-1} collected during 2000 combined with an earlier preliminary version of the analysis of the data collected at $\sqrt{s}$ = 189–202 GeV [27]. This paper appears in the proceedings of the Sixth International Workshop on Tau Lepton Physics. At this conference, held in Victoria, B.C., Canada, I presented the results of the DELPHI search for charged Higgs bosons. The analysis presented in paper V [25] uses the full data sample collected during the last year of running combined with the results presented in paper III. No excess was found and the charged Higgs boson mass limit was set at 73.8 GeV/c^2 at 95% confidence level independently of the branching ratios of the charged Higgs boson (see region F in Figure 5.1).

CHAPTER 6

Outlook

The DELPHI detector is not the only place where charged Higgs bosons have been searched for. The four detectors at the LEP collider have all been used for searching for charged Higgs bosons.

After the closure of the LEP collider the search will continue at other colliders. There are at the moment searches going on using the detectors at the Tevatron collider at Fermilab and preparations have started for the searches that will take place at the Large Hadron Collider that is presently being constructed at CERN.

6.1 ALEPH, L3 and OPAL

The results of the search for charged Higgs bosons presented in this thesis are confirmed by the searches performed at the other detectors at the LEP collider. The observed and expected mass limits for the existence of a charged Higgs boson obtained by the four collaborations are listed in Table 6.1.

The L3 collaboration has observed an excess in the reconstructed mass distribution in the hadronic and semileptonic channels around 68 GeV/c^2 [29]. This excess is however too small to be compatible with the the cross section for pair production of charged Higgs bosons predicted by the 2HDM. When treated as a fluctuation of the expected background the excess prevents the L3 collaboration from excluding the existence of charged Higgs bosons with masses larger than 67.1 GeV/c^2 at 95% confidence level. The excess observed by the L3 collaboration is not confirmed by the other experiments.

TABLE 6.1. The observed and expected mass limits for charged Higgs bosons from the searches performed at the four detectors at the LEP collider, and the limits obtained when combining the results from the four detectors. All limits are given at 95% confidence level.

Detector	Observed limit	Expected limit
ALEPH [28]	78.0 GeV/c^2	76.9 GeV/c^2
DELPHI	73.8 GeV/c^2	75.4 GeV/c^2
L3 [29]	67.1 GeV/c^2	75.0 GeV/c^2
OPAL [30]	72.2 GeV/c^2	74.5 GeV/c^2
Combined [31]	78.5 GeV/c^2	78.9 GeV/c^2

The mass limits obtained from the searches performed at the detectors at the LEP collider are sensitive to the limited sizes of the collected data samples. By combining the data collected by the four detectors, an integrated luminosity four times that collected by one of the detectors alone can be achieved. Such a combined analysis has been done by the LEP working group for Higgs boson searches [31]. The result of the combined analysis excludes the existence of charged Higgs bosons with masses lower than 78.5 GeV/c^2 at 95% confidence level independently of the branching ratios of the charged Higgs boson (see Figure 6.1).

6.2 The Tevatron at Fermilab

The Tevatron collider at the Fermi National Accelerator Laboratory outside Chicago, Illinois, is a proton antiproton collider. Two general purpose detectors, called CDF and D0, are collecting data at this collider.

The energy of the proton antiproton collisions is high enough to allow $t\bar{t}$ quark pairs to be created. If $m_{\mathrm{H}^\pm} < m_t$ these t quarks can decay into charged Higgs bosons ($t \longrightarrow \mathrm{H}^+ + b$). In a 2HDM of type II the branching ratio for this process is proportional to $m_b^2 \tan^2\beta + m_t^2 \cot^2\beta$. This branching ratio is large for small and large values of $\tan\beta$ but has a minimum at $\tan\beta = \sqrt{m_t/m_b} \approx 7.5$, where the search for charged Higgs bosons is difficult.

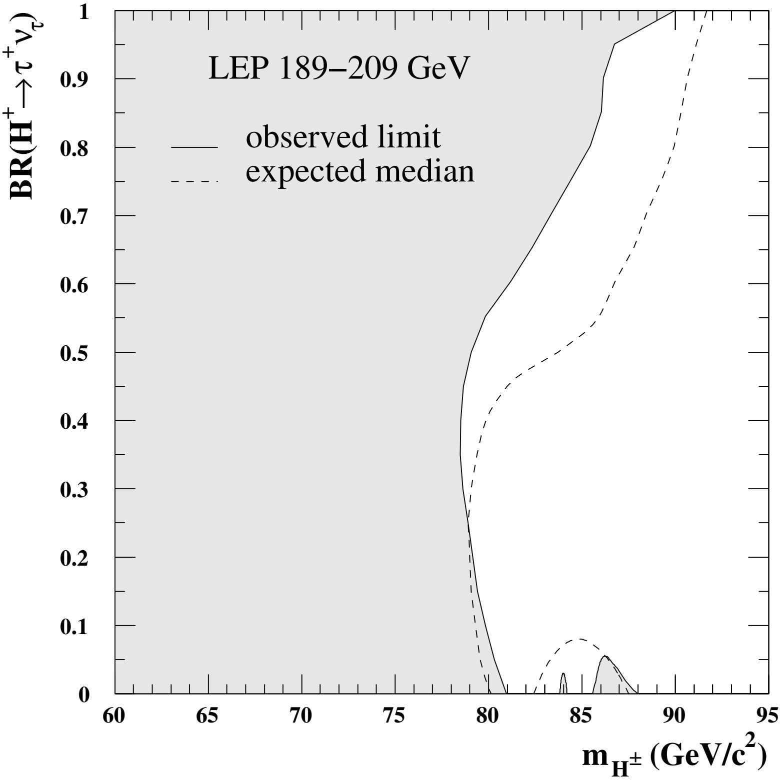

Figure 6.1. The observed and expected mass limits for charged Higgs bosons obtained when combining the results of the four detectors at the LEP collider [31]. The limits are given at 95% confidence level.

During run I of the Tevatron in 1992–1996 the D0 detector collected about 110 pb^{-1} of data at $\sqrt{s} = 1.8$ TeV. The analysis of these data resulted in that the existence of a charged Higgs boson was excluded at 95% confidence level in the regions of the parameter space spanned by $\tan\beta$ and $m_{\mathrm{H}^\pm}$ that have been marked 'I' in Figure 6.2 [32].

Run IIa of the Tevatron is scheduled to take place in 2001–2002. During this run the D0 detector will collect approx. 2 fb^{-1} of data at

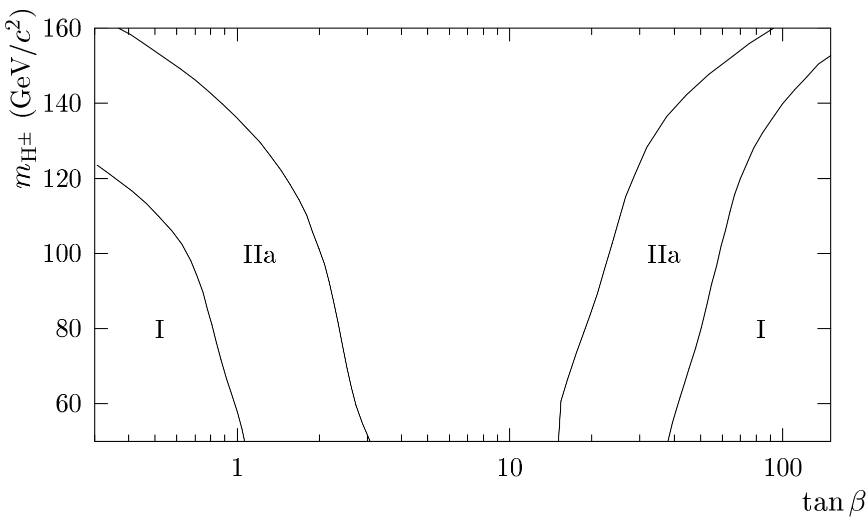

FIGURE 6.2. The regions in the $(\tan\beta,\ m_{H^\pm})$ plane that have been excluded at 95% confidence level by the search for charged Higgs bosons in t quark decays at the D0 detector using the data collected during run I of the Tevatron and the regions expected to be excluded using the data collected during run IIa if no excess with respect to the background expectation will be observed.

$\sqrt{s} = 2$ TeV. If no signal will be observed, the new data are expected to exclude the regions marked 'IIa' in Figure 6.2 at 95% confidence level [33].

6.3 The Large Hadron Collider at CERN

The Large Hadron Collider (LHC) is a proton proton collider that is presently being built at CERN. The new collider will have a centre of mass energy of 14 TeV and the first particle collisions are scheduled to take place in 2007. Two general purpose detectors are being constructed at the LHC. They are called ATLAS and CMS.

At the LHC, there are several potential sources for production of charged Higgs bosons. A few of them have been considered to be promising for searches. If the charged Higgs boson is lighter than the

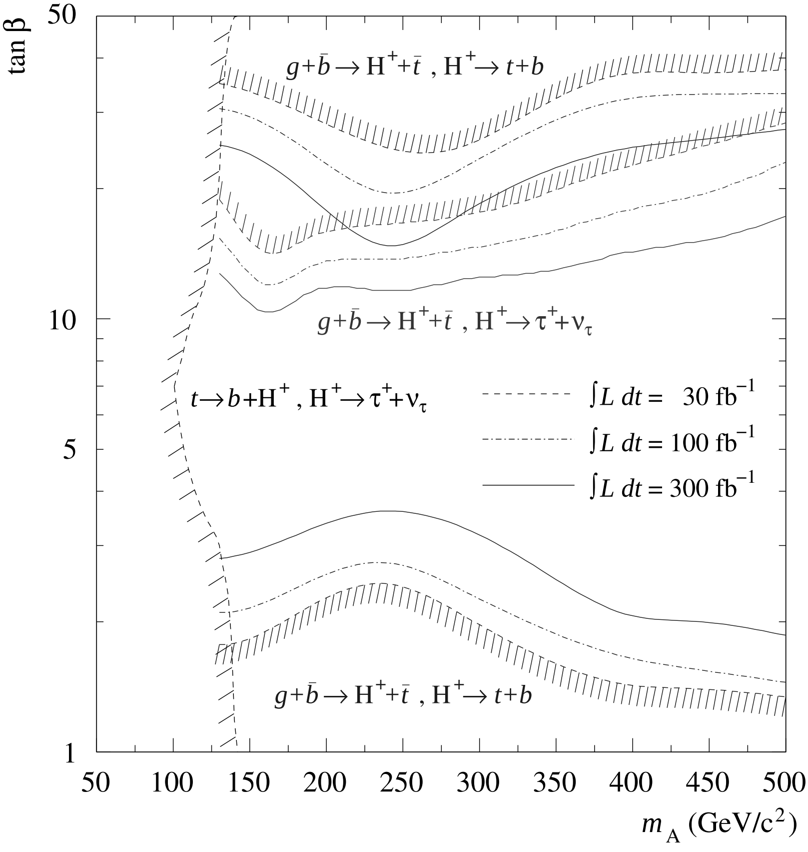

Figure 6.3. The discovery potential for charged Higgs bosons in the different production and decay channels that have been studied by the ATLAS collaboration. The results are presented as the regions in the MSSM parameter space (m_{A}, $\tan\beta$) where a charged Higgs boson can be discovered using data collected by the ATLAS detector with an integrated luminosity of 30, 100 and 300 fb^{-1} respectively.

t quark, many charged Higgs bosons will be produced in the decays of the $t\bar{t}$ quarks pairs produced in the proton proton collisions. If the charged Higgs boson is heavier than the t quark, it can be produced via gluon-b fusion ($g + \bar{b} \longrightarrow \mathrm{H}^+ + \bar{t}$).

The discovery potential for charged Higgs bosons in the ATLAS detector in the different production and decay channels that have been studied by the ATLAS collaboration are shown in Figure 6.3 [34, 35]. The results of the studies are presented as the regions in the MSSM parameter space (m_{A}, $\tan\beta$) where a charged Higgs boson can be discovered using data collected by the ATLAS detector.

CHAPTER 7

Acknowledgements

First of all I would like to thank is my thesis supervisor professor Tord Ekelöf for his encouragement and support.

I would also like to thank Rémi Silvestre who at the time I joined the DELPHI collaboration had been conducting the search for charged Higgs bosons within the collaboration. The computer code I inherited from him was a great help in starting to understand the DELPHI analysis software.

I wish to thank the members of the group responsible for the search for charged Higgs bosons within the DELPHI collaboration: Ari Kiiskinen, Guillelmo Gómez-Ceballos, Pierre Lutz, Marco Battaglia and Francisco Matorras.

Many thanks to Kristina Gunne at Swedish office at CERN for all the help with many practical details during my stays in Geneva.

I would also like to thank the residents at the Foyer International des Étudiants Saint Justin in Geneva for making my stays memorable. I especially would like to thank Jens Vang for initiating many game playing sessions.

I would like to thank Yann Coadou for his input on the chapter on the charged Higgs boson searches at D0 and ATLAS.

During the five years I have been a Ph.D. student I have met many new colleagues and made many new friends. A special thank you goes to Fredrik Tegenfeldt, Jérôme Damet, Jan Conrad, Rikard Enberg, Nicuşor Tîmneanu, Inken Koch, Maria Gunther Axelsson, Mattias Lantz and all the other Ph.D. student for making the Department of Radiation Sciences at Uppsala University a really good place to be.

APPENDIX A

The Standard Model

The Standard Model is a description of the elementary particles and their interactions based on quantum field theory [36, 37]. By requiring that the predictions of the model should be invariant under a set of local gauge transformations, a number of gauge fields must be included in the theory. These gauge fields are responsible for the interactions between the fermion fields. In this way the photon field, responsible for the electromagnetic interaction, and the $W^{\pm}$ and Z^0 boson fields, responsible for the weak interaction, emerge as a consequence of invariance under the $SU(2)_L$ and $U(1)_Y$ local gauge transformations. In the same way the gluon fields responsible for the strong interaction emerge from $SU(3)_c$ invariance.

A.1 $SU(2)_L$ and $U(1)_Y$

The Lagrangian density describing a massless non-interacting charged lepton field $\psi^\ell(x)$ and its associated neutrino field $\psi^\nu(x)$ is given by

$$\mathcal{L}_F = i(\bar{\psi}^\ell \partial\!\!\!/ \psi^\ell + \bar{\psi}^\nu \partial\!\!\!/ \psi^\nu) \ . \tag{A.1}$$

In order for the model to be able to describe the parity violation observed in the weak interaction the fermion fields must be decomposed into their left-handed and right-handed components:

$$\psi_L(x) = \frac{1}{2}(1-\gamma_5)\psi(x) \tag{A.2}$$

$$\psi_R(x) = \frac{1}{2}(1+\gamma_5)\psi(x) \ . \tag{A.3}$$

The weak interaction couples the left-handed charged lepton field to the left-handed neutrino field. These fields are therefore grouped into a weak isospin doublet ($T = \frac{1}{2}$, $\mathbf{T} = \frac{1}{2}\boldsymbol{\sigma}$):

$$\Psi_L^\ell(x) = \begin{pmatrix} \psi_L^\nu(x) \\ \psi_L^\ell(x) \end{pmatrix} . \tag{A.4}$$

The right-handed fields are not affected by the weak interaction and are left as weak isospin singlets[1] ($T = 0$). Using this notation the Lagrangian density can be written

$$\mathcal{L}_F = i(\bar{\Psi}_L^\ell \partial\!\!\!/ \Psi_L^\ell + \bar{\psi}_R^\ell \partial\!\!\!/ \psi_R^\ell + \bar{\psi}_R^\nu \partial\!\!\!/ \psi_R^\nu) . \tag{A.5}$$

This Lagrangian density is invariant under the global gauge transformations of the $\mathrm{SU}(2)_L$ group,

$$\Psi_L(x) \overset{\mathrm{SU}(2)_L}{\longrightarrow} e^{\frac{1}{2}ig\boldsymbol{\sigma}\cdot\boldsymbol{\omega}}\Psi_L(x) \tag{A.6}$$

$$\psi_R(x) \overset{\mathrm{SU}(2)_L}{\longrightarrow} \psi_R(x) , \tag{A.7}$$

as well as of the $\mathrm{U}(1)_Y$ group,

$$\Psi_L(x) \overset{\mathrm{U}(1)_Y}{\longrightarrow} e^{ig'Y\alpha}\Psi_L(x) \tag{A.8}$$

$$\psi_R(x) \overset{\mathrm{U}(1)_Y}{\longrightarrow} e^{ig'Y\alpha}\psi_R(x) , \tag{A.9}$$

where the hypercharge Y is the mean electric charge of the members of the multiplet[2], i.e. $-\frac{1}{2}$, -1 and 0 for $\Psi_L^\ell(x)$, $\psi_R^\ell(x)$ and $\psi_R^\nu(x)$ respectively, g and g' are the coupling constants and $\boldsymbol{\omega}$ and α are arbitrary constants. From this definition of the hypercharge follows that the electric charge of a field is given by

$$Q = Y + T_{(3)} , \tag{A.10}$$

where $T_{(3)}$ is the third component of the weak isospin.

[1] The right-handed neutrino field has so far not been experimentally observed and is sometimes excluded from the theory.

[2] Different conventions for the definition of the hypercharge exist. Another common alternative convention defines the hypercharge as twice the value used here.

If the condition of gauge invariance is tightened so that the Lagrangian density is required to be invariant also when these transformations are locally defined, i.e. when $\boldsymbol{\omega}(x)$ and $\alpha(x)$ are arbitrary functions of space and time,

$$\Psi_L(x) \xrightarrow{\mathrm{SU(2)}_L} e^{\frac{1}{2}ig\boldsymbol{\sigma}\cdot\boldsymbol{\omega}(x)}\Psi_L(x) \tag{A.11}$$

$$\psi_R(x) \xrightarrow{\mathrm{SU(2)}_L} \psi_R(x) \tag{A.12}$$

$$\Psi_L(x) \xrightarrow{\mathrm{U(1)}_Y} e^{ig'Y\alpha(x)}\Psi_L(x) \tag{A.13}$$

$$\psi_R(x) \xrightarrow{\mathrm{U(1)}_Y} e^{ig'Y\alpha(x)}\psi_R(x) \ , \tag{A.14}$$

then the partial derivatives ∂^μ must be replaced by the so called covariant derivatives D^μ,

$$D^\mu = \partial^\mu + \frac{1}{2}ig\boldsymbol{\sigma}\cdot\mathbf{W}^\mu + ig'YB^\mu \quad \text{(for doublets)} \tag{A.15}$$

$$D^\mu = \partial^\mu + ig'YB^\mu \quad \text{(for singlets)} \ , \tag{A.16}$$

where the gauge fields $\mathbf{W}^\mu(x)$ and $B^\mu(x)$ transform under the gauge transformations in such a way that the additional terms that appear in the transformed Lagrangian density are compensated:

$$\begin{aligned}\frac{1}{2}\boldsymbol{\sigma}\cdot\mathbf{W}^\mu(x) \xrightarrow{\mathrm{SU(2)}_L}\ & e^{\frac{1}{2}ig\boldsymbol{\sigma}\cdot\boldsymbol{\omega}(x)}\,\frac{1}{2}\boldsymbol{\sigma}\cdot\mathbf{W}^\mu(x)\,e^{-\frac{1}{2}ig\boldsymbol{\sigma}\cdot\boldsymbol{\omega}(x)} \\ & + \frac{i}{g}\left(\partial^\mu e^{\frac{1}{2}ig\boldsymbol{\sigma}\cdot\boldsymbol{\omega}(x)}\right)e^{-\frac{1}{2}ig\boldsymbol{\sigma}\cdot\boldsymbol{\omega}(x)}\end{aligned} \tag{A.17}$$

$$B^\mu(x) \xrightarrow{\mathrm{SU(2)}_L} B^\mu(x) \tag{A.18}$$

$$\mathbf{W}^\mu(x) \xrightarrow{\mathrm{U(1)}_Y} \mathbf{W}^\mu(x) \tag{A.19}$$

$$B^\mu(x) \xrightarrow{\mathrm{U(1)}_Y} B^\mu(x) - \partial^\mu\alpha(x) \ . \tag{A.20}$$

After replacing the partial derivatives with the covariant derivatives the fermionic Lagrangian density describes the free lepton fields and the interaction between the lepton fields and the gauge fields:

$$\mathcal{L}_F = i(\bar{\Psi}^\ell_L \not{D}\Psi^\ell_L + \bar{\psi}^\ell_R \not{D}\psi^\ell_R + \bar{\psi}^\nu_R \not{D}\psi^\nu_R) \ . \tag{A.21}$$

A.2 The Higgs Mechanism

The Lagrangian density describing the free gauge fields in the absence of fermions is given by

$$\mathcal{L}_B = -\frac{1}{4}\mathbf{W}^{\mu\nu}\cdot\mathbf{W}_{\mu\nu} - \frac{1}{4}B^{\mu\nu}B_{\mu\nu} \ , \tag{A.22}$$

where

$$\mathbf{W}^{\mu\nu}(x) = \partial^\nu\mathbf{W}^\mu(x) - \partial^\mu\mathbf{W}^\nu(x) + g\mathbf{W}^\mu(x)\times\mathbf{W}^\nu(x) \tag{A.23}$$

$$B^{\mu\nu}(x) = \partial^\nu B^\mu(x) - \partial^\mu B^\nu(x) \ . \tag{A.24}$$

The last term in the expression for $\mathbf{W}^{\mu\nu}(x)$ (A.23) has been added in order to make the Lagrangian density (A.22) invariant under the $\mathrm{SU}(2)_L$ gauge transformation (A.17).

The gauge fields described by the Lagrangian density (A.22) are massless. However, since the $\mathrm{W}^\pm$ and Z^0 boson fields of the weak interaction are massive, this equation can not be a complete description of these fields. Unfortunately a mass term proportional to $\mathbf{W}^\mu\cdot\mathbf{W}_\mu$ can not be added to the Lagrangian density since such a term would not be invariant under the local gauge transformations. In order to explain the heavy masses of the weak interaction boson fields in a way that does not violate gauge invariance, additional fields (Higgs fields) are introduced in the theory. The interaction with these fields is responsible for generating the masses of the weak interaction bosons.

Two complex scalar Higgs fields, $\phi^+(x)$ and $\phi^0(x)$, are added to the theory and grouped together into a weak isospin doublet in the same way as the left-handed leptons:

$$\Phi(x) = \begin{pmatrix} \phi^+(x) \\ \phi^0(x) \end{pmatrix} \ . \tag{A.25}$$

This field transforms under the $\mathrm{SU}(2)_L$ and $\mathrm{U}(1)_Y$ transformation in the same way as the left-handed lepton fields (see equations A.11 and A.13), but with hypercharge $Y = \frac{1}{2}$. The self-interaction of the field is given by the so called Higgs potential:

$$V(\Phi) = \mu^2\Phi^\dagger\Phi + \lambda(\Phi^\dagger\Phi)^2 \ , \tag{A.26}$$

where $\lambda > 0$ and $\mu^2 < 0$.

After adding the free field term of the Higgs field (where the partial derivative has been replaced by the covariant derivative to ensure gauge invariance) as well as the terms resulting from the Higgs potential to the Lagrangian density it takes the form

$$\begin{aligned}\mathcal{L}_B = & -\frac{1}{4}\mathbf{W}^{\mu\nu}\cdot\mathbf{W}_{\mu\nu} - \frac{1}{4}B^{\mu\nu}B_{\mu\nu} \\ & + (D^\mu\Phi)^\dagger(D_\mu\Phi) - \mu^2\Phi^\dagger\Phi - \lambda(\Phi^\dagger\Phi)^2 \ . \end{aligned} \tag{A.27}$$

The vacuum state (i.e. the state with the lowest possible energy) is degenerate for the Higgs potential. There are infinitely many possible vacuum states. These can be written as

$$\Phi^{(0)}(x) = e^{\frac{1}{2}i\boldsymbol{\sigma}\cdot\boldsymbol{\theta}}\frac{1}{\sqrt{2}}\begin{pmatrix} 0 \\ v \end{pmatrix} , \tag{A.28}$$

where the so called vacuum expectation value (v.e.v.) is given by

$$v \equiv \sqrt{-\frac{\mu^2}{\lambda}} \ . \tag{A.29}$$

The Lagrangian density is invariant under the $\mathrm{SU}(2)_L$ transformations, but the vacuum states are not. This is an example of spontaneous symmetry breaking.

Since all possible vacuum states are equivalent (any two of them can be connected by a gauge transformation) the choice $\boldsymbol{\theta} = 0$ can be made. Expanding the Higgs field around this vacuum state gives:

$$\begin{aligned}\Phi(x) &= e^{\frac{1}{2}i\boldsymbol{\sigma}\cdot 2\boldsymbol{\eta}(x)/v}\frac{1}{\sqrt{2}}\begin{pmatrix} 0 \\ v + h(x) \end{pmatrix} \\ &\approx \frac{1}{\sqrt{2}}\begin{pmatrix} \eta_2(x) + i\eta_1(x) \\ v + h(x) - i\eta_3(x) \end{pmatrix} \ . \end{aligned} \tag{A.30}$$

The three real so called Goldstone fields $\boldsymbol{\eta}(x)$ can be removed from the theory by a suitable gauge transformation. The gauge where the Goldstone fields are zero is called the unitary gauge.

Transformed to the unitary gauge the Lagrangian density takes the form

$$
\begin{aligned}
\mathcal{L}_B = & -\frac{1}{4}\mathbf{W}^{\mu\nu}\cdot\mathbf{W}_{\mu\nu} - \frac{1}{4}B^{\mu\nu}B_{\mu\nu} \\
& + \frac{1}{2}\left[\begin{pmatrix} 0 & v+h \end{pmatrix}\left(\overleftarrow{\partial^{\mu}} - \frac{1}{2}ig\boldsymbol{\sigma}\cdot\mathbf{W}^{\mu} - \frac{1}{2}ig'B^{\mu}\right)\right] \\
& \qquad \left[\left(\overrightarrow{\partial_{\mu}} + \frac{1}{2}ig\boldsymbol{\sigma}\cdot\mathbf{W}_{\mu} + \frac{1}{2}ig'B_{\mu}\right)\begin{pmatrix} 0 \\ v+h \end{pmatrix}\right] \\
& + \frac{1}{2}\lambda v^2(v+h)^2 - \frac{1}{4}\lambda(v+h)^4 \\
= & -\frac{1}{4}\mathbf{W}^{\mu\nu}\cdot\mathbf{W}_{\mu\nu} - \frac{1}{4}B^{\mu\nu}B_{\mu\nu} + \frac{1}{2}(\partial^{\mu}h)(\partial_{\mu}h) \\
& + \left(\frac{1}{8}g^2\mathbf{W}^{\mu}\cdot\mathbf{W}_{\mu} + \frac{1}{8}g'^2B^{\mu}B_{\mu} - \frac{1}{4}gg'W^{\mu}_{(3)}B_{\mu}\right)(v+h)^2 \\
& + \frac{1}{2}\lambda v^2(v+h)^2 - \frac{1}{4}\lambda(v+h)^4 \ . \qquad \text{(A.31)}
\end{aligned}
$$

Since this expression contains a term mixing the $B^{\mu}(x)$ and $W^{\mu}_{(3)}(x)$ fields these fields are not mass eigenstates. By diagonalising the mass matrix the mass eigenstates can be found:

$$Z^{\mu}(x) = \cos\theta_{\mathrm{w}}W^{\mu}_{(3)}(x) - \sin\theta_{\mathrm{w}}B^{\mu}(x) \qquad \text{(A.32)}$$

$$A^{\mu}(x) = \sin\theta_{\mathrm{w}}W^{\mu}_{(3)}(x) + \cos\theta_{\mathrm{w}}B^{\mu}(x) \ , \qquad \text{(A.33)}$$

where

$$\tan\theta_{\mathrm{w}} = \frac{g'}{g} \ . \qquad \text{(A.34)}$$

If the remaining components of the $\mathbf{W}^{\mu}(x)$ field are rearranged into a complex scalar field:

$$W^{\mu}(x) = \frac{1}{\sqrt{2}}(W^{\mu}_{(1)}(x) - iW^{\mu}_{(2)}(x)) \ , \qquad \text{(A.35)}$$

and

$$W^{\mu\nu}(x) = \partial^{\nu}W^{\mu}(x) - \partial^{\mu}W^{\nu}(x) \qquad \text{(A.36)}$$

$$Z^{\mu\nu}(x) = \partial^\nu Z^\mu(x) - \partial^\mu Z^\nu(x) \tag{A.37}$$

$$A^{\mu\nu}(x) = \partial^\nu A^\mu(x) - \partial^\mu A^\nu(x) \tag{A.38}$$

then the Lagrangian takes the form

$$\begin{aligned}
\mathcal{L}_B = & -\frac{1}{2}W^{\mu\nu\dagger}W_{\mu\nu} + m_{\mathrm{W}^\pm}^2 W^{\mu\dagger}W_\mu \\
& -\frac{1}{4}Z^{\mu\nu}Z_{\mu\nu} + \frac{1}{2}m_{\mathrm{Z}^0}^2 Z^\mu Z_\mu \\
& -\frac{1}{4}A^{\mu\nu}A_{\mu\nu} \\
& +\frac{1}{2}(\partial^\mu h)(\partial_\mu h) - \frac{1}{2}m_{\mathrm{h}^0}^2 h^2 \\
& + ig\cos\theta_{\mathrm{w}}((W^{\mu\dagger}W^\nu - W^{\nu\dagger}W^\mu)\partial_\mu Z_\nu + \\
& \qquad (\partial^\mu W^\nu - \partial^\nu W^\mu)W_\nu^\dagger Z_\mu - (\partial^\mu W^{\nu\dagger} - \partial^\nu W^{\mu\dagger})W_\nu Z_\mu) \\
& + ie((W^{\mu\dagger}W^\nu - W^{\nu\dagger}W^\mu)\partial_\mu A_\nu + \\
& \qquad (\partial^\mu W^\nu - \partial^\nu W^\mu)W_\nu^\dagger A_\mu - (\partial^\mu W^{\nu\dagger} - \partial^\nu W^{\mu\dagger})W_\nu A_\mu) \\
& + g^2\cos^2\theta_{\mathrm{w}}(W^{\mu\dagger}W^\nu Z_\mu Z_\nu - W^{\mu\dagger}W_\mu Z^\nu Z_\nu) \\
& + e^2(W^{\mu\dagger}W^\nu A_\mu A_\nu - W^{\mu\dagger}W_\mu A^\nu A_\nu) \\
& + eg\cos\theta_{\mathrm{w}}(W^{\mu\dagger}W^\nu(Z_\mu A_\nu + A_\mu Z_\nu) - 2W^{\mu\dagger}W_\mu A^\nu Z_\nu) \\
& + \frac{g^2}{2}W^{\mu\dagger}W^\nu(W_\mu^\dagger W_\nu - W_\nu^\dagger W_\mu) \\
& + \frac{g^2 v}{2}W^{\mu\dagger}W_\mu h + \frac{g^2}{4}W^{\mu\dagger}W_\mu h^2 \\
& + \frac{g^2 v}{4\cos^2\theta_{\mathrm{w}}}Z^\mu Z_\mu h + \frac{g^2}{8\cos^2\theta_{\mathrm{w}}}Z^\mu Z_\mu h^2 \\
& - \lambda v h^3 - \frac{\lambda}{4}h^4 + \frac{\lambda v^4}{4}\ ,
\end{aligned} \tag{A.39}$$

where

$$m_{\mathrm{W}^\pm} = \frac{gv}{2} \tag{A.40}$$

$$m_{\mathrm{Z}^0} = \frac{gv}{2\cos\theta_{\mathrm{w}}} \tag{A.41}$$

$$m_{\mathrm{h}^0} = \sqrt{2\lambda}\, v = \sqrt{-2\mu^2} \tag{A.42}$$

and

$$e = g\sin\theta_{\mathrm{w}} = g'\cos\theta_{\mathrm{w}} \ . \tag{A.43}$$

The first four lines in the transformed bosonic Lagrangian density (A.39) describe the free fields of the charged $\mathrm{W}^{\pm}$ boson, the neutral Z^0 boson, the photon and a neutral scalar boson called the Higgs boson, with masses $m_{\mathrm{W}^{\pm}}$, m_{Z^0}, 0 and m_{h^0} respectively. The remaining terms describe interactions between these fields. The very last term is a constant that can be dropped without changing the predictions of the theory.

The recipe described above for transforming a theory with massless interaction bosons into a theory with massive interaction bosons using spontaneous symmetry breaking is called the Higgs mechanism. It should be noted that the number of independent states (or degrees of freedom) does not change due to this transformation.

The original theory contained four massless vector fields each having two possible polarisation states and two complex scalar Higgs fields each having two degrees of freedom. After the spontaneous symmetry breaking there are three massive vector boson fields with three possible polarisation states each, one massless vector field having two possible polarisation states and one real scalar Higgs field having one degree of freedom. The total number of independent states is twelve in both cases.

A.3 Three Generations of Leptons and Quarks

The quarks can be included in the model by adding a quark term to the fermionic Lagrangian density (A.21) of the same form as the lepton term[3]:

$$\begin{aligned} \mathcal{L}_F &= i(\bar{\Psi}^{\ell}_L \not{D} \Psi^{\ell}_L + \bar{\psi}^{\ell}_R \not{D} \psi^{\ell}_R + \bar{\psi}^{\nu}_R \not{D} \psi^{\nu}_R) \\ &\quad + i(\bar{\Psi}^{q}_L \not{D} \Psi^{q}_L + \bar{\psi}^{\kappa}_R \not{D} \psi^{\kappa}_R + \bar{\psi}^{\alpha}_R \not{D} \psi^{\alpha}_R) \ , \end{aligned} \tag{A.44}$$

[3]here α is short for $\acute{\alpha}\nu\omega$ meaning above, and κ is short for $\kappa\acute{\alpha}\tau\omega$ meaning below.

where

$$\Psi_L^q(x) = \begin{pmatrix} \psi_L^\alpha(x) \\ \psi_L^\kappa(x) \end{pmatrix} . \tag{A.45}$$

The quark fields' hypercharges are $Y = \frac{1}{6}$, $\frac{2}{3}$ and $-\frac{1}{3}$ for $\Psi_L^q(x)$, $\psi_R^\alpha(x)$ and $\psi_R^\kappa(x)$ respectively.

In the Lagrangian density given above the fermion fields are massless. If a mass term of the form

$$-m\bar{\psi}\psi = -m(\bar{\psi}_L\psi_R + \bar{\psi}_R\psi_L) \tag{A.46}$$

is added to the Lagrangian density it would become non-invariant under the gauge transformations. Instead non-zero masses for the fermions can be achieved by adding a set of gauge invariant terms that couple the fermion fields to the Higgs doublet:

$$\begin{aligned}\mathcal{L}_F = {} & i(\bar{\Psi}_L^\ell \not{D}\Psi_L^\ell + \bar{\psi}_R^\ell \not{D}\psi_R^\ell + \bar{\psi}_R^\nu \not{D}\psi_R^\nu) \\ & - g_\ell(\bar{\Psi}_L^\ell \psi_R^\ell \Phi + \Phi^\dagger \bar{\psi}_R^\ell \Psi_L^\ell) - g_\nu(\bar{\Psi}_L^\ell \psi_R^\nu \tilde{\Phi} + \tilde{\Phi}^\dagger \bar{\psi}_R^\nu \Psi_L^\ell) \\ & + i(\bar{\Psi}_L^q \not{D}\Psi_L^q + \bar{\psi}_R^\kappa \not{D}\psi_R^\kappa + \bar{\psi}_R^\alpha \not{D}\psi_R^\alpha) \\ & - g_\kappa(\bar{\Psi}_L^q \psi_R^\kappa \Phi + \Phi^\dagger \bar{\psi}_R^\kappa \Psi_L^q) - g_\alpha(\bar{\Psi}_L^q \psi_R^\alpha \tilde{\Phi} + \tilde{\Phi}^\dagger \bar{\psi}_R^\alpha \Psi_L^q) ,\end{aligned} \tag{A.47}$$

where

$$\tilde{\Phi}(x) = i\sigma_2\Phi^*(x) = \begin{pmatrix} \phi^{0*}(x) \\ -\phi^-(x) \end{pmatrix} \tag{A.48}$$

is the charge conjugate of $\Phi(x)$ with hypercharge $Y = -\frac{1}{2}$. Writing this expression in the unitary gauge results in

$$\begin{aligned}\mathcal{L}_F = {} & \bar{\psi}^\ell(i\not{\partial} - m_\ell)\psi^\ell + \bar{\psi}^\nu(i\not{\partial} - m_\nu)\psi^\nu \\ & + \bar{\psi}^\kappa(i\not{\partial} - m_\kappa)\psi^\kappa + \bar{\psi}^\alpha(i\not{\partial} - m_\alpha)\psi^\alpha \\ & + \text{interaction terms} ,\end{aligned} \tag{A.49}$$

where

$$m_f = \frac{g_f v}{\sqrt{2}} \;\; ; \; f = \ell,\ \nu,\ \kappa,\ \alpha , \tag{A.50}$$

i.e. the masses of the fermions are proportional to the coupling strengths between the fermion fields and the Higgs field and to the vacuum expectation value of the Higgs field.

The above expression only contains the fields from one fermion generation. By letting the fermion fields of the same type from different generations span a vector space,

$$\Psi_L^F(x) = \begin{pmatrix} \Psi_L^{f_1}(x) \\ \Psi_L^{f_2}(x) \\ \Psi_L^{f_3}(x) \end{pmatrix} \; ; \; (F,f) = (L,\ell),\ (Q,q) \tag{A.51}$$

$$\psi_R^F(x) = \begin{pmatrix} \psi_R^{f_1}(x) \\ \psi_R^{f_2}(x) \\ \psi_R^{f_3}(x) \end{pmatrix} \; ; \; (F,f) = (L,\ell),\ (N,\nu),\ (K,\kappa),\ (A,\alpha) \; , \tag{A.52}$$

the fermionic Lagrangian density (A.47) can be generalised to take into account the three known fermion generations and to include terms that couple fields from different generations:

$$\begin{aligned} \mathcal{L}_F = {} & i(\bar{\Psi}_L^L \not{D} \Psi_L^L + \bar{\psi}_R^L \not{D} \psi_R^L + \bar{\psi}_R^N \not{D} \psi_R^N) \\ & - \bar{\Psi}_L^L G^L \psi_R^L \Phi - \Phi^\dagger \bar{\psi}_R^L G^L \Psi_L^L \\ & - \bar{\Psi}_L^L G^N \psi_R^N \tilde{\Phi} - \tilde{\Phi}^\dagger \bar{\psi}_R^N G^N \Psi_L^L \\ & + i(\bar{\Psi}_L^Q \not{D} \Psi_L^Q + \bar{\psi}_R^K \not{D} \psi_R^K + \bar{\psi}_R^A \not{D} \psi_R^A) \\ & - \bar{\Psi}_L^Q G^K \psi_R^K \Phi - \Phi^\dagger \bar{\psi}_R^K G^K \Psi_L^Q \\ & - \bar{\Psi}_L^Q G^A \psi_R^A \tilde{\Phi} - \tilde{\Phi}^\dagger \bar{\psi}_R^A G^A \Psi_L^Q \; , \end{aligned} \tag{A.53}$$

where G^L, G^N, G^K and G^A are 3×3 Hermitian coupling matrices.

The mass eigenstates can be found by diagonalising the resulting mass matrices:

$$M^F = \frac{v}{\sqrt{2}} G^F \; . \tag{A.54}$$

If U^F are the unitary matrices diagonalising M^F, i.e. if

$$\hat{M}^F = U^F M^F U^{F\dagger} \tag{A.55}$$

are diagonal matrices containing the mass eigenvalues of the fermions, then the corresponding mass eigenstates (flavours) can be written as

$$\hat{\psi}^F(x) = U^F \psi^F(x) \ . \tag{A.56}$$

Since the matrices diagonalising the different fermion spaces are different, the weak isospin partner of a mass eigenstate is not a mass eigenstate, but a linear combination of mass eigenstates. For this reason only one of the components of each weak isospin doublet can be chosen as a mass eigenstate. By convention this is the $T_{(3)} = -\frac{1}{2}$ component for the leptons and the $T_{(3)} = \frac{1}{2}$ component for the quarks. The common mass and weak isospin eigenstates for the charged leptons are labelled e (electron), μ (muon) and τ (tauon). The weak isospin eigenstates for the neutral leptons are labelled ν_e, ν_μ and ν_τ and the mass eigenstates are labelled ν_1, ν_2 and ν_3. The weak isospin eigenstates can be written as linear combinations of the mass eigenstates:

$$\begin{pmatrix} \psi^{\nu_e}(x) \\ \psi^{\nu_\mu}(x) \\ \psi^{\nu_\tau}(x) \end{pmatrix} = \begin{pmatrix} U_{e1} & U_{e2} & U_{e3} \\ U_{\mu 1} & U_{\mu 2} & U_{\mu 3} \\ U_{\tau 1} & U_{\tau 2} & U_{\tau 3} \end{pmatrix} \begin{pmatrix} \psi^{\nu_1}(x) \\ \psi^{\nu_2}(x) \\ \psi^{\nu_3}(x) \end{pmatrix} , \tag{A.57}$$

where

$$U = U^L U^{N\dagger} \tag{A.58}$$

is the neutrino mixing matrix[4].

The common mass and weak isospin eigenstates for the up-type (α) quarks are labelled u (up), c (charm) and t (top). The mass eigenstates of the down-type (κ) quarks are labelled d (down), s (strange) and b (bottom) and the weak isospin eigenstates are labelled d', s' and b'. Again, the weak isospin eigenstates can be written as linear combinations of the mass eigenstates:

$$\begin{pmatrix} \psi^{d'}(x) \\ \psi^{s'}(x) \\ \psi^{b'}(x) \end{pmatrix} = \begin{pmatrix} V_{ud} & V_{us} & V_{ub} \\ V_{cd} & V_{cs} & V_{cb} \\ V_{td} & V_{ts} & V_{tb} \end{pmatrix} \begin{pmatrix} \psi^{d}(x) \\ \psi^{s}(x) \\ \psi^{b}(x) \end{pmatrix} , \tag{A.59}$$

[4]If the right-handed neutrinos are excluded from the model, the terms containing the G^N couplings are absent from the Lagrangian density (A.53) and the masses of the neutrinos are zero. In this case the neutrino mixing matrix can be taken as the unit matrix and there is no mixing between the neutrino generations.

where

$$V = U^A U^{K\dagger} \tag{A.60}$$

is the Cabibbo-Kobayashi-Maskawa (CKM) quark mixing matrix.

The mixing matrices are unitary and can contain complex elements. The presence of complex elements can provide an explanation to why the combined charge conjugation and parity symmetry (CP) has been observed to be violated in the decay of neutral kaons.

Writing the fermionic Lagrangian density (A.53) in the unitary gauge using mass eigenstates (dropping the hats in the notation) results in

$$\begin{aligned}
\mathcal{L}_F = {} & \bar{\psi}^L(i\not{\partial} - M^L)\psi^L + \bar{\psi}^N(i\not{\partial} - M^N)\psi^N \\
& + \bar{\psi}^K(i\not{\partial} - M^K)\psi^K + \bar{\psi}^A(i\not{\partial} - M^A)\psi^A \\
& + e\bar{\psi}^L \not{A}\psi^L - \frac{2}{3}\, e\bar{\psi}^A \not{A}\psi^A + \frac{1}{3}\, e\bar{\psi}^K \not{A}\psi^K \\
& - \frac{g}{2\sqrt{2}}(\bar{\psi}^N U^\dagger \not{W}(1-\gamma_5)\psi^L + \bar{\psi}^L \not{W}^\dagger(1-\gamma_5)U\psi^N) \\
& - \frac{g}{2\sqrt{2}}(\bar{\psi}^A \not{W}(1-\gamma_5)V\psi^K + \bar{\psi}^K V^\dagger \not{W}^\dagger(1-\gamma_5)\psi^A) \\
& - \frac{g}{4\cos\theta_{\mathrm{w}}}\bar{\psi}^N \not{Z}(1-\gamma_5)\psi^N \\
& + \frac{g}{4\cos\theta_{\mathrm{w}}}\bar{\psi}^L \not{Z}(1 - 4\sin^2\theta_{\mathrm{w}} - \gamma_5)\psi^L \\
& - \frac{g}{4\cos\theta_{\mathrm{w}}}\bar{\psi}^A \not{Z}\left(1 - \frac{8}{3}\sin^2\theta_{\mathrm{w}} - \gamma_5\right)\psi^A \\
& + \frac{g}{4\cos\theta_{\mathrm{w}}}\bar{\psi}^K \not{Z}\left(1 - \frac{4}{3}\sin^2\theta_{\mathrm{w}} - \gamma_5\right)\psi^K \\
& - \frac{1}{v}\,\bar{\psi}^L M^L \psi^L h - \frac{1}{v}\,\bar{\psi}^N M^N \psi^N h \\
& - \frac{1}{v}\,\bar{\psi}^K M^K \psi^K h - \frac{1}{v}\,\bar{\psi}^A M^A \psi^A h \ .
\end{aligned} \tag{A.61}$$

The first four terms describe the free fields of the charged and neutral leptons and of the up-type (α) and down-type (κ) quarks. The remaining terms describe interactions.

The complete Lagrangian density describing the unified electromagnetic and weak interactions (the so called electroweak interaction) is given by the sum of the bosonic (A.39) and fermionic (A.61) Lagrangian densities.

In this Lagrangian the $\mathrm{SU}(2)_L$ and $\mathrm{U}(1)_Y$ symmetries present in the original theory has been hidden due to the spontaneous symmetry breaking in the Higgs mechanism. The new Lagrangian is however symmetric under the $\mathrm{U}(1)_{\mathrm{em}}$ symmetry

$$\phi(x) \stackrel{\mathrm{U}(1)_{\mathrm{em}}}{\longrightarrow} e^{ieQ\alpha(x)}\phi(x) \tag{A.62}$$

of the electromagnetic interaction. This implies that the electric charge is conserved.

Since in the fermion mass matrices M^F and the corresponding matrices describing the coupling between fermions and the Higgs field G^F can be diagonalised simultaneously, there are no terms in the Lagrangian density describing any coupling between a neutral boson field and two fermion fields with different flavour. This absence of so called flavour changing neutral currents is confirmed by experimental measurements.

A.4 $\mathrm{SU}(3)_c$

In order to explain how the flavours and spins assigned to the constituent quarks of e.g. the Δ^{++}, Δ^- and Ω^- baryons can be compatible with the Pauli exclusion principle[5] an additional quantum number is assigned to the quark fields. This quantum number, called colour charge, can take one of three possible values, called red (r), green (g) and blue (b). The colour charges has nothing to do with ordinary colours, but the name has been established due to an analogy with the fundamental colours used in additive colour imaging, where the sum of red, green and blue light appears as white to the observer of e.g. a television screen. In the same way the sum of one red, one green and one blue colour charge is zero. Continuing this analogy a particle or group of particles with a total colour charge of zero is called colourless or white.

Quark fields of the same flavour with different colours are arranged

[5]The Pauli exclusion principle states that two fermions cannot have the same set of eigenvalues for all quantum numbers.

in a colour triplet:

$$\Psi^q(x) = \begin{pmatrix} \psi_r^q(x) \\ \psi_g^q(x) \\ \psi_b^q(x) \end{pmatrix} . \tag{A.63}$$

The Lagrangian density is invariant under the global gauge transformations of the $\mathrm{SU}(3)_c$ group,

$$\Psi^q(x) \xrightarrow{\mathrm{SU}(3)_c} e^{ig_s \sum_{k=1}^{8} \lambda_k T_k} \Psi^q(x) , \tag{A.64}$$

where the eight linearly independent traceless Hermitian 3×3 matrices T_k are the generators of rotations in $\mathrm{SU}(3)_c$ space, g_s is the coupling constant and the eight λ_k's are arbitrary real numbers.

By requiring that the Lagrangian density should be invariant also when this transformation is locally defined, i.e. when the $\lambda_k(x)$'s are arbitrary functions of space and time, eight massless gauge fields must be introduced into the theory. These fields are called gluon fields and are the interaction boson fields of the strong interaction.

The gluon fields themselves have colour charges and interact with each other. A consequence of this self-interaction is that the strength of the strong interaction is not inversely proportional to the distance between the interacting fermions, which is the normal behaviour for interactions mediated by gauge boson fields without self-interactions (like e.g. the electromagnetic interaction mediated by the photon field). Instead the strength of the strong interaction for large distances increases linearly with distance. From this follows that the energy needed to permanently separate two colour charges is infinite. For this reason the quarks cluster in groups with a total colour charge of zero. Such groups can consist of one quark and one anti-quark (mesons) or of three quarks (baryons). The phenomenon that quarks are never found as free particles but only as parts of colourless clusters is called confinement.

A.5 Feynman Rules and Feynman Diagrams

The quantum field equations that can be derived from the Standard Model Lagrangian density can not be solved exactly. This means that approximations must be used in order to make theoretical predictions from the model. The most commonly used technique for making such approximations is perturbation theory.

When applying perturbation theory the Lagrangian density is divided into two parts. The first part, $\mathcal{L}_0(x)$, contains the terms describing the free (non-interacting) particle fields and the second part, $\mathcal{L}_I(x)$, contains the terms describing the interactions between these fields:

$$\mathcal{L}(x) = \mathcal{L}_0(x) + \mathcal{L}_I(x) \ . \tag{A.65}$$

The quantum field equations derived from the free particle field Lagrangian density alone, neglecting the interaction part, can be solved, giving a set of free particle solutions. The interaction part is then considered to give rise to perturbations that cause transitions between these free particle states.

The probability for a transition between an initial state $|i\rangle$ and a final state $|j\rangle$ is related to the so called S matrix element:

$$P(|i\rangle \longrightarrow |j\rangle) = |\langle j|S|i\rangle|^2 = |S_{ji}|^2 \ , \tag{A.66}$$

where

$$S = e^{i\int \mathcal{L}_I(x) d^4x} \ . \tag{A.67}$$

When the expression for S is expanded as a Taylor series the matrix element can be calculated. If the coupling constants in the interaction Lagrangian density are small the series is convergent and more and more accurate results can be obtained by computing additional terms in the series. However, the complexity of the calculations increases dramatically for each new term. For many processes involving the strong interaction the $\mathrm{SU}(3)_c$ coupling constant is too large and the series diverges. In this case other non-perturbative approximation methods must be used.

In the perturbative case, the S matrix element can be calculated using the Feynman rules. When using these rules the matrix element is written in terms of a so called Feynman amplitude, $\mathcal{M}$:

$$\begin{aligned} S_{ji} = \delta_{ji} + (2\pi)^4 \delta^4 &\left(\sum_j p'_j - \sum_i p_i \right) \\ &\prod_i \sqrt{\frac{1}{2VE_i}} \prod_j \sqrt{\frac{1}{2VE'_j}} \prod_f \sqrt{2m_f}\, \mathcal{M} \ , \end{aligned} \tag{A.68}$$

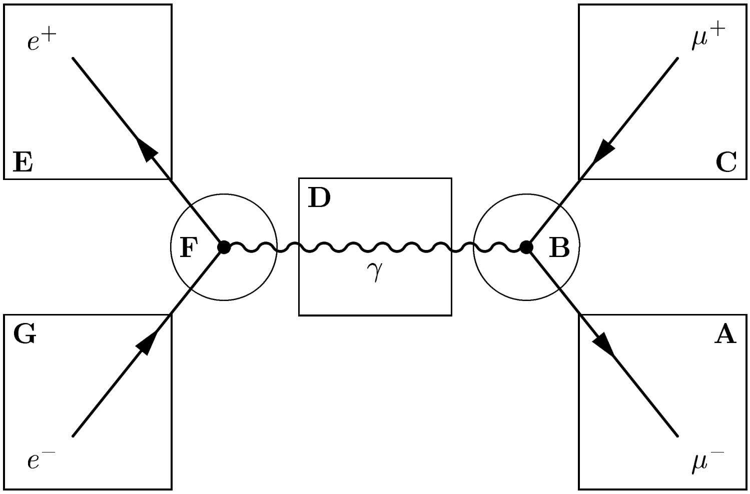

$$\mathcal{M} = \boxed{\overset{\mathbf{A}}{\bar{u}^{\mu}_{r'_1}(\mathbf{p}'_1)}}\ \overset{\mathbf{B}}{ie\gamma^{\alpha}}\ \boxed{\overset{\mathbf{C}}{v^{\mu}_{r'_2}(\mathbf{p}'_2)}}\ \boxed{\overset{\mathbf{D}}{\frac{-ig_{\alpha\beta}}{k^2+i\varepsilon}}}\ \boxed{\overset{\mathbf{E}}{\bar{v}^{e}_{r_2}(\mathbf{p}_2)}}\ \overset{\mathbf{F}}{ie\gamma^{\beta}}\ \boxed{\overset{\mathbf{G}}{u^{e}_{r_1}(\mathbf{p}_1)}}$$

FIGURE A.1. Example demonstrating the use of Feynman diagrams and the application of Feynman rules. The figure shows the Feynman diagram for the reaction $e^+ + e^- \longrightarrow \gamma \longrightarrow \mu^+ + \mu^-$ as well as the expression for the corresponding Feynman amplitude $\mathcal{M}$ derived by applying the Feynman rules to the diagram. The correspondence between the different parts of the diagram and the different factors in the amplitude has been indicated in the figure by labelled boxes and circles. The electron (positron) momentum and polarisation are p_1 and r_1 (p_2 and r_2). The muon (anti-muon) momentum and polarisation are p'_1 and r'_1 (p'_2 and r'_2). The momentum of the intermediate photon is k. From energy and momentum conservation follows that $p_1 + p_2 = k = p'_1 + p'_2$.

where $p_i = (E_i, \mathbf{p}_i)$ are the four-momenta of the particles in the initial state, $p'_j = (E'_j, \mathbf{p}'_j)$ are the four-momenta of the particles in the final state, and V is the normalisation volume for the particle states. The index i runs over all particles present in the initial state, j runs over all particles present in the final state and f runs over all fermions present in the initial or the final state.

The Feynman amplitude $\mathcal{M}$ is a sum of contributions from all channels having the same initial and final states. E.g. when calculating the Feynman amplitude for the reaction $e^+ + e^- \longrightarrow \mu^+ + \mu^-$ in lowest order, the contributions from the three channels $e^+ + e^- \longrightarrow \gamma \longrightarrow \mu^+ + \mu^-$, $e^+ + e^- \longrightarrow \mathrm{Z}^0 \longrightarrow \mu^+ + \mu^-$ and $e^+ + e^- \longrightarrow \mathrm{h}^0 \longrightarrow \mu^+ + \mu^-$ must be added together. In order to calculate higher order terms additional channels involving loops must be included.

When calculating the contribution to the Feynman amplitude from a given reaction channel, a graphical representation of the Feynman rules can make the calculations easier. After drawing this so called Feynman diagram depicting the interaction channel, the contribution to the Feynman amplitude can be derived by applying a set of rules to the diagram. According to these rules each part of the diagram corresponds to a factor in the amplitude. These factors can be derived from the Lagrangian density. A fermion in the initial or final state is represented by a four-spinor, $u_r(\mathbf{p})$ or $v_r(\mathbf{p})$, a boson in the initial or final state is represented by its polarisation vector $\varepsilon(\mathbf{k})$ and particles in intermediate states are represented by so called propagators, i.e. Green's function solutions to the free field quantum field equations. The factors representing different types of vertices can be derived from the corresponding term in $\mathcal{L}_I(x)$. An example of the application of the Feynman rules to a Feynman diagram is shown in Figure A.1.

The Feynman diagrams needed to calculate the lowest order in the expansion do not contain any loops, and can be compared to a tree with roots and branches. The lowest order calculations are therefore sometimes called to be 'tree level'.

From the calculated transition probabilities predictions can be made for a number of measurable quantities like cross sections and branching ratios. The cross section for a process where two particles with four-momenta p_1 and p_2 collide and create a set of particles with four-momenta p'_j is

$$\sigma = \int (2\pi)^4 \delta^4 \left(\sum_j p'_j - p_1 - p_2 \right) \frac{1}{4\sqrt{(p_1 p_2)^2 - m_1^2 m_2^2}} \prod_j \left(\frac{d^3\mathbf{p}'_j}{(2\pi)^3 2E'_j} \right) \prod_f (2m_f) \; |\mathcal{M}|^2 \;, \tag{A.69}$$

and the decay rate of a particle with four-momentum p into a set of particles with four-momenta p'_j is

$$\Gamma_j = \int (2\pi)^4 \delta^4 \left(\sum_j p'_j - p \right) \frac{1}{2E} \prod_j \left(\frac{d^3 \mathbf{p}'_j}{(2\pi)^3 2E'_j} \right) \prod_f (2m_f) \, |\mathcal{M}|^2 \, . \tag{A.70}$$

The branching ratio for a decay channel is the fraction of the total number of decays that goes into that particular channel, i.e.

$$\mathrm{BR}(j) = \frac{\Gamma_j}{\Gamma} = \frac{\Gamma_j}{\sum_k \Gamma_k} \, , \tag{A.71}$$

where the sum is taken over all possible final states to which the particle can decay.

When performing calculations with the help of the Feynman rules, many of the resulting integrals do not have finite solutions. However, the theory can give physically interpretable results if these infinities are removed in a consistent way. This process, called renormalisation, involves redefining the coupling constants and the particle masses after calculating each order of perturbation. The procedure hides the infinities in the unmeasurable 'bare' charges of the theory, while the physical or 'screened' charges remain finite. After renormalisation the predictions from the theory are finite and can be compared to experimental results.

References

[1] John F. Gunion, Howard E. Haber, Gordon L. Kane and Sally Dawson, *The Higgs Hunter's Guide*, Perseus Publishing, Cambridge, Massachusetts, 1990, ISBN 0-7382-0305-X.

[2] Sheldon L. Glashow and Steven Weinberg, Natural Conservation Laws for Neutral Currents, Phys. Rev. **D15** (1977) 1958.

[3] T. D. Lee, A Theory of Spontaneous T Violation, Phys. Rev. **D8** (1973) 1226–1239.

[4] Yue-Liang Wu and Lincoln Wolfenstein, Sources of CP Violation in the Two-Higgs-Doublet Model, Phys. Rev. Lett. **73** (1994) 1762–1764.

[5] Howard Georgi, A Model of Soft CP Violation, Hadronic J. **1** (1978) 155.

[6] M. Carena and P. M. Zervas, Higgs Physics, in *Physics at LEP2*, edited by G. Altarelli, T. Sjöstrand and F. Zwirner, volume 1, pages 351–462, 1996, ISSN 0007-8328, ISBN 92-9083-081-6.

[7] Yuval Grossman, Phenomenology of models with more than two Higgs doublets, Nucl. Phys. **B426** (1994) 355–384.

[8] D. E. Groom *et al.*, Review of Particle Physics, Eur. Phys. J. **C15** (2000) 1, available on the PDG WWW pages (http://pdg.lbl.gov).

[9] John F. Gunion and Howard E. Haber, Higgs Bosons in Supersymmetric Models — 1, Nucl. Phys. **B272** (1986) 1.

[10] DELPHI Collaboration, P. Aarnio *et al.*, The DELPHI detector at LEP, Nucl. Instrum. Meth. **A303** (1991) 233–276.

[11] DELPHI Collaboration, P. Abreu *et al.*, Performance of the DELPHI detector, Nucl. Instrum. Meth. **A378** (1996) 57–100.

[12] G. Gómez-Ceballos and F. Matorras, τ polarisation at LEP 2 — Application to Searches, DELPHI 98-63 PHYS 784, DELPHI Collaboration, 1998.

[13] R. A. Fisher, The Use of Multiple Measurements in Taxionomic Problems, Annals of Eugenics **7** (1936) 179–188.

[14] W. J. Murray, Improved B tagging using Impact Paramters, DELPHI 95-167 PHYS 581, DELPHI Collaboration, 1995.

[15] M. Battaglia and D. Liko, Identification of hadronic final states in W decays by jet flavour tagging and determination of BR$(W \longrightarrow cs)$/BR$(W \longrightarrow q\bar{q})$, DELPHI 97-68 PHYS 714, DELPHI Collaboration, 1997.

[16] V. F. Obraztsov, Confidence limits for processes with small statistics in several subchannels and with measurement errors, Nucl. Instrum. Meth. **A316** (1992) 388–390.

[17] A. L. Read, Optimal Statistical Analysis of Search Results Based on the Likelihood Ratio and its Application to the Search for the MSM Higgs Boson at $\sqrt{s}$ = 161 and $\sqrt{s}$ = 172 GeV, DELPHI 97-158 PHYS 737, DELPHI Collaboration, 1997.

[18] DELPHI Collaboration, P. Abreu *et al.*, Search for pair-produced heavy scalars in Z^0 decays, Z. Phys. **C64** (1994) 183–194.

[19] DELPHI Collaboration, W. Adam *et al.*, Search for pair production of heavy objects in 4-jet events at $\sqrt{s}$ = 130–136 GeV, Z. Phys. **C73** (1996) 1–9.

[20] DELPHI Collaboration, P. Abreu *et al.*, Search for neutral and charged Higgs bosons in e^+e^- collisions at $\sqrt{s}$ = 161 GeV and 172 GeV, Eur. Phys. J. **C2** (1998) 1–37.

[21] Rémi Silvestre, *Recherche des bosons de Higgs chargés à LEP2 avec le détecteur DELPHI*, Ph.D. thesis, Université Louis Pasteur, Strasbourg, 1997.

[22] DELPHI Collaboration, P. Abreu *et al.*, Search for charged Higgs bosons in e^+e^- collisions at $\sqrt{s} = 172$ GeV, Phys. Lett. **B420** (1998) 140–156.

[23] DELPHI Collaboration, P. Abreu *et al.*, Search for Charged Higgs Bosons at LEP 2, Phys. Lett. **B460** (1999) 484–497.

[24] DELPHI Collaboration, P. Abreu *et al.*, Search for Charged Higgs Bosons in e^+e^- Collisions at $\sqrt{s} = 189$–202 GeV, to be submitted to Phys. Lett. **B**.

[25] M. Battaglia *et al.*, Search for Charged Higgs Bosons in e^+e^- Collisions at $\sqrt{s} = 189$–208 GeV, contributed paper to the XXXVI$^{\text{th}}$ Rencontres de Moriond, Les Arcs, France, 10–17 March 2001, DELPHI 2001-030 CONF 471.

[26] Mattias Ellert *et al.*, Search for Charged Higgs Bosons in e^+e^- Collisions at DELPHI, in *TAU 2000*, proceedings of the Sixth International Workshop on Tau Lepton Physics, Victoria, B.C., Canada, 18–21 September 2000, to appear in Nucl. Phys. **B**, Proc. Suppl.

[27] M. Battaglia *et al.*, Search for Charged Higgs Bosons in e^+e^- Collisions at $\sqrt{s} = 189$–202 GeV, contributed paper to the XXX$^{\text{th}}$ International Conference on High Energy Physics, Osaka, Japan, 27 July–2 August 2000.

[28] ALEPH Collaboration, Update of the search for charged Higgs bosons for Year 2001 winter conferences, contributed paper to the XXXVI$^{\text{th}}$ Rencontres de Moriond, Les Arcs, France, 10–17 March 2001, ALEPH 2001-016 CONF 2001-013.

[29] L3 Collaboration, Search for Charged Higgs Bosons in e^+e^- Collisions at Centre-of-Mass Energies up to 209 GeV, contributed paper to the XXXVI$^{\text{th}}$ Rencontres de Moriond, Les Arcs, France, 10–17 March 2001, L3 note 2643.

[30] The OPAL Higgs Working Group, Searches for Higgs Bosons in Extensions to the Standard Model in e^+e^- Collisions at the Highest LEP Energies, contributed paper to the XXXVI$^{\text{th}}$ Rencontres de Moriond, Les Arcs, France, 10–17 March 2001, OPAL Physics Note PN472.

[31] The LEP working group for Higgs boson searches, Search for Charged Higgs Boson: Preliminary combined results using LEP data collected at energies up to 209 GeV, contributed paper to the XXXVI$^{\mathrm{th}}$ Rencontres de Moriond, Les Arcs, France, 10–17 March 2001, LHWG internal note 2001-1.

[32] D0 Collaboration, B. Abbott *et al.*, Search for charged Higgs bosons in decays of top quark pairs, Phys. Rev. Lett. **82** (1999) 4975–4980.

[33] Dhiman Chakraborty, Charged Higgs Bosons, in *Report of the Tevatron Higgs Working Group*, edited by Marcela Carena, John S. Conway, Hower E. Haber and John D Hobbs, 2000, hep-ph/0010338.

[34] ATLAS Detector and Physics Performance, Technical Design Report, ATLAS Collaboration, 25 May 1999, CERN/LHCC/99-15, ATLAS TDR 15.

[35] Kétévi Adiklè Assamagan and Yann Coadou, The Hadronic τ Decay of a Heavy H^+ in ATLAS, ATLAS PHYS-2000-032, ATLAS Collaboration, 2000.

[36] F. Mandl and G. Shaw, *Quantum Field Theory*, John Wiley and Sons, Chichester, Revised edition, 1984, ISBN 0 471 94186 7.

[37] L. B. Okun, *Leptons and Quarks*, North-Holland, Amsterdam, 1982, ISBN 0 444 86924 7.